

Extreme paleoceanographic conditions in a Paleozoic oceanic upwelling system: Organic productivity and widespread phosphogenesis in the Permian Phosphoria Sea

Eric E. Hiatt*

Department of Geology, University of Wisconsin, 800 Algoma Boulevard, Oshkosh, Wisconsin 54901, USA

David A. Budd

Department of Geological Sciences, University of Colorado, Boulder, Colorado 80309-0399, USA

ABSTRACT

High-resolution geochemical data from phosphorites and associated lithofacies of the Permian Phosphoria Rock Complex suggest that organic matter deposition and phosphogenesis occurred in fundamentally different oceanographic conditions than those of modern oceanic upwelling systems. Unlike modern phosphorites, those of the Phosphoria accumulated in a shallow marginal sea within a semi-restricted epicontinental embayment that extended landward into proximal environments bordered by evaporative lagoons. The Phosphoria Rock Complex phosphorites formed in outer ramp (<200 m water depth), organically productive mid-ramp, and very shallow and restricted inner-ramp environments. Chemostratigraphic data (total organic carbon, sulfur, phosphate, $\delta^{13}\text{C}_{\text{PO}_4\text{-CO}_3}$, Ni, Cr, and Cd) indicate that this wide range of paleoenvironments was largely dysoxic or anoxic; euxinic conditions developed sporadically. High cadmium and nickel concentrations suggest maximum paleoproductivity (preserved total organic carbon up to 15 wt%) was associated with anoxic and euxinic conditions. Water column oxygen and trophic levels are interpreted to have been the primary controls over macrofaunal distribution in the Phosphoria, not cold-water temperatures as has been previously inferred.

These findings, augmented by recent Permian paleoclimate and ocean circulation models, suggest that an oxygen-poor, nutrient-rich intermediate water mass flowed into the Phosphoria embayment and impinged on the mid-ramp area. Seasonal coastal upwelling brought this water to the surface, where it mixed with warm waters flowing seaward from the restricted shallow lagoons in west-central Wyoming, resulting in high paleoproductivity and organic matter accumulation and oxygen depletion in the water column. Warming of the waters on the broad, shallow ramp, coupled with seasonal attenuation of the coastal upwelling system, is predicted to have led to a positive feedback between productivity and phosphogenesis through a wide range of environments. This new model and our findings illustrate that paleoceanographic setting and paleoenvironment must be taken into account to fully understand the geochemical variation seen in ancient phosphorites.

Keywords: Phosphoria, upwelling, chemostratigraphy, chemofacies, phosphorite, paleoceanography.

*Corresponding author: hiatt@uwosh.edu.

INTRODUCTION

The Phosphoria Rock Complex contains one of the largest sedimentary phosphate deposits in the geologic record (e.g., Cook and McElhinny, 1979). This series of phosphorite-siltstone-chert-carbonate-evaporite successions was deposited in the “Phosphoria Sea” on the western margin of North America during the Permian (Fig. 1). The Phosphoria Rock Complex contains more than five times the total mass of phosphorus in today’s oceans (McKelvey et al., 1953); an estimated 1.7×10^{12} metric tons of P_2O_5 were originally deposited (Cathcart et al., 1984). Organic carbon concentrations can exceed 15 wt% (Maughan, 1994; Hiatt, 1997), and 31×10^9 metric tons of petroleum have been generated (Claypool et al., 1978). The Phosphoria Rock Complex is truly an example of an extreme sedimentary system.

The Phosphoria Rock Complex also spans one of the most extraordinary global climate transitions in earth history (Fig. 2). The Early Permian was marked by widespread glaciation in the southern hemisphere (Pennsylvanian to Early Permian), low CO_2 levels, and probably widespread sea ice at the North Pole (Barron and Fawcett, 1995). In contrast, the Late Permian marks the onset of hot and dry climates over most of the middle and low-latitude continents, rapidly increasing CO_2 levels (two to five times modern values; Berner, 1994), widespread desert environments with vast areas of evaporite deposition (Ziegler, 1990; Zarkov, 1984), and widespread anoxic deep-water conditions in the world’s oceans (Wignall and Twitchett, 1996; Knoll et al., 1995). In contrast to Early Permian glaciation, the southern continents in the Late Permian were marked by warm, high-latitude climates that brought boreal forests, coal swamps, and reptiles within 10° of the South Pole (Taylor et al., 1992; Dickins, 1984, 1996; Rees et al., 1999).

The abundance of phosphate, organic matter, and chert in the Phosphoria Rock Complex has long been cited as evidence for a coastal upwelling system in the Phosphoria Sea (e.g., McKelvey et al., 1959; Sheldon, 1989). Upwelling is also predicted by phosphate and elemental mass balance calculations (Piper and Link, 2002), atmospheric circulation models (Parrish, 1982; Kutzbach and Ziegler, 1994), and paleowind directions that suggest a net offshore movement of surface waters by Ekman transport (Sheldon et al., 1967; Parrish and Peterson, 1988). There is no doubt that upwelling-associated biological productivity led to the deposition of organic matter and phosphate in the Phosphoria Rock Complex.

Although the existence of an oceanic upwelling system in the Phosphoria Sea is considered a certainty, many unanswered questions remain concerning the oceanographic conditions that led to these extreme sedimentary deposits. As Boyd (1993, p. 183) pointed out, “A completely satisfying explanation for the origin of the phosphatic members has yet to appear.” Key unanswered questions are: What was the nature (oxygen and nutrient levels, primarily) of the upwelled water? Under what oceanographic conditions did sedimentary phosphate form? And, what role did the semi-restricted nature of this embayment play in the oceanography of the Phosphoria Sea?

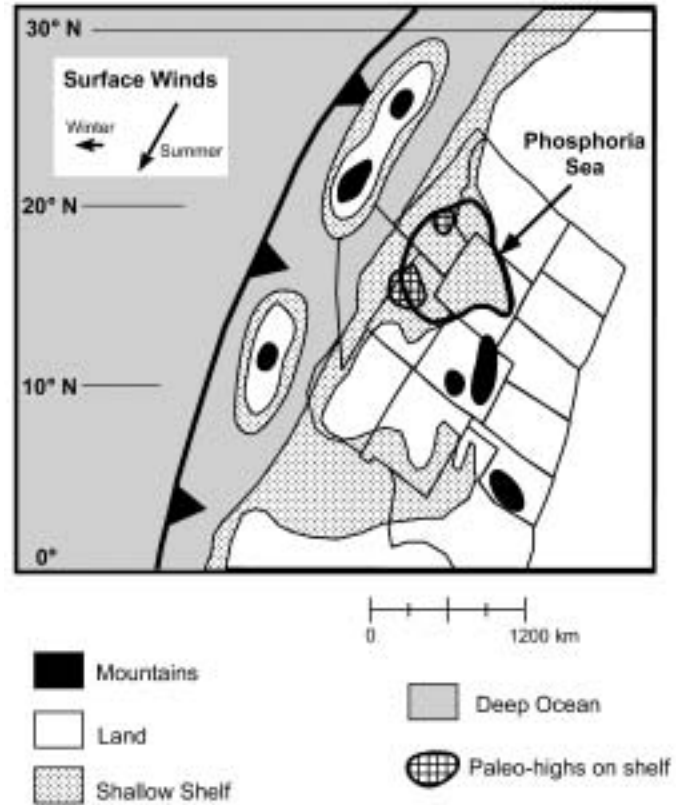


Figure 1. Position of Phosphoria Sea in context of Late Permian plate tectonic reconstruction of western North American continent and eastern Panthalassa Ocean. Position of paleoshoreline represents sea-level high-stand. Paleowind vectors are based on Kutzbach and Ziegler (1994); wind strengths (inset box) are 5.0 and 1.8 m/s for summer and winter, respectively. Approximate positions of paleohighs on the Wyoming paleoshelf are from Skipp and Hall (1980) and Wardlaw (1977). Map is modified from Scotese and Langford (1995).

We believe that answers to these questions have been hindered by attempts to make the Phosphoria Rock Complex “fit” a model based on the modern Peru margin—a model that involves upwelling of cold ($0\text{--}10^\circ\text{C}$), nutrient-rich deep water onto a steep and narrow continental shelf (e.g., McKelvey et al., 1953, 1959; Sheldon, 1963, 1984; Parrish, 1982; Wardlaw and Collinson, 1984). The applicability of this interpretation to the Phosphoria Rock Complex has been bolstered by the presence of faunal elements that are interpreted as representing cold-water, “Arctic” conditions in the Phosphoria Sea (Wardlaw, 1980; Wardlaw et al., 1995).

In the last 20 years, research on the modern ocean and the Phosphoria Rock Complex has resulted in a somewhat different view of these enigmatic rocks. It now appears that the Phosphoria Sea was a relatively shallow (<200 m), semi-isolated epicontinental basin (Ketner, 1977; Scotese and Langford, 1995). Paleoclimate models suggest mean summer air temperatures over the shallow, marginal Phosphoria Sea were as high as $30\text{--}45^\circ\text{C}$

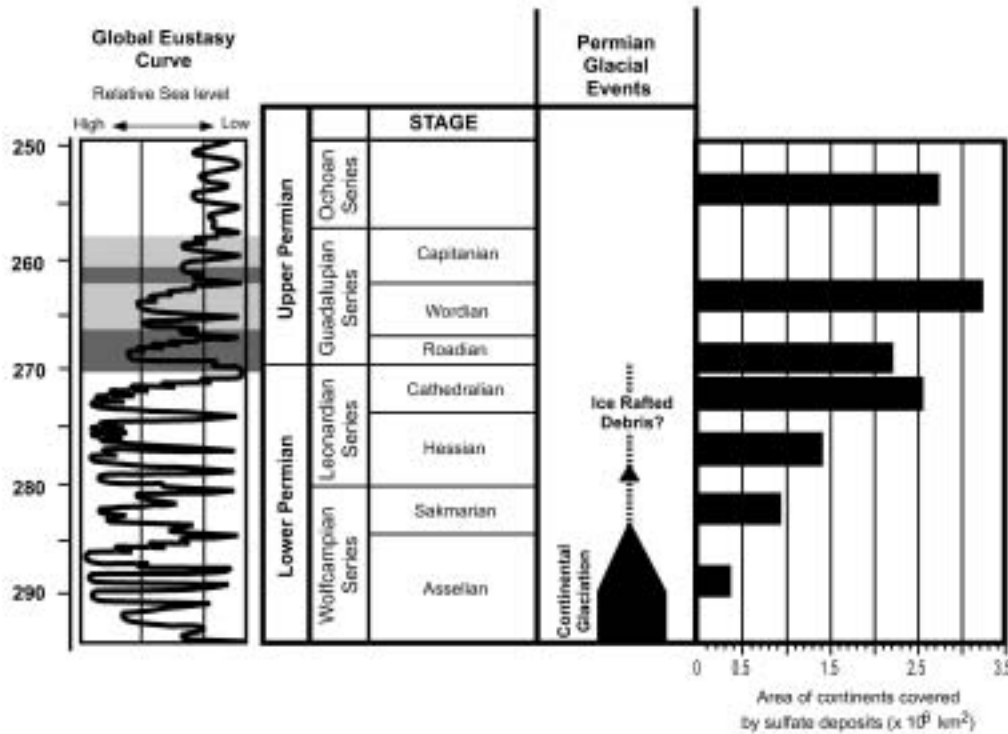


Figure 2. Permian Series and Stage names for southwestern United States and global eustasy curve; eustasy curve records sea-level variations with amplitudes of ~200 m (modified from Ross and Ross, 1994). Shaded zone on eustasy curve represents Phosphoria Rock Complex, and darkly shaded zones represent intervals of phosphate-rich Meade Peak (lower zone) and Retort (upper zone) deposition. Relative extents of Permian glacial events are shown in middle right column (width of black area provides an estimate of possible ice sheet extent; evidence for ice sheets extending to the earliest Sakmarian from González-Bonorino and Eyles (1995) and Dickins (1996); evidence for ice sheets in South Africa in Artinskian from Visser, 1996; evidence for ice-rafted debris from Frakes et al. (1992). Extent of global evaporite deposits as sulfate minerals (anhydrite and gypsum) is shown by bar graph at right (data from Zharkov, 1984).

(Kutzbach and Ziegler, 1994; Barron and Fawcett, 1995). Phosphogenesis, which is the precipitation of phosphate from seawater at or just below the sediment-water interface, occurred not only in the deeper portions of the basin, but also in shallower, inner-shelf settings (Sheldon, 1984; Peterson, 1984; Hiatt, 1997; Trappe, 1998; Stephens and Carroll, 1999; Hendrix and Byers, 2000). Paleotemperatures ranged from temperate (14–26 °C; mean of 21 °C) at sites of maximum phosphogenesis to warm (34–37 °C) across the shallow paleoshelf (Hiatt and Budd, 2001). Elevated salinities and stratification of the water column have also been proposed (Hite, 1978; Dahl et al., 1993; Stephens and Carroll, 1999). Piper and Link (2002), however, argued for temperature rather than salinity stratification. Based on the lower, phosphorite-rich portion of the Meade Peak member and mass balance calculations, Piper and Link (2002) determined that the Phosphoria Sea was “sediment-starved” and that, based on analogies with modern ocean basins, biological productivity was only moderately high. Piper (2001) used concentrations of Cd, Mo, Zn, Cu, and perhaps Ni as further evidence of elevated biological productivity in the Meade Peak member, and he coupled these with other trace elements, such as Cr, V, and U to further suggest that the Phosphoria Sea was marked by anoxic, denitrifying, but not sulfate-reducing bottom waters during deposition of this lower Meade Peak interval. Piper (2001) and Piper and Link (2002), however, did not analyze their data in a stratigraphic and regional framework. This leads to the question: How did oceanographic conditions vary regionally or temporally (stratigraphically) during the life of the upwelling system? In addition, no one

has directly studied the relationship between paleoecology and chemostratigraphy of the Meade Peak to test whether the paleontologic data support either the salinity or temperature stratification model.

All of these recent findings and the fundamental unanswered questions that remain suggest it is time to reassess the nature of the original upwelling model of the Phosphoria Sea. Here, the geochemical and macrofaunal data from the Meade Peak member of the Phosphoria Formation are presented in a stratigraphic and regional framework that further clarifies the relationship between paleoproductivity, chemofacies, phosphogenesis, and oceanographic setting.

THE PHOSPHORIA ROCK COMPLEX

Deposition of the Phosphoria Rock Complex occurred in the “Phosphoria Sea” (Fig. 1), which formed in a shallow marginal foreland basin on the western margin of North America at a paleolatitude of about 20°N (Scotese and Langford, 1995). The Phosphoria Sea was partially separated from the Panthalassa Ocean by an island arc system (e.g., Scotese and Langford, 1995). The Phosphoria Rock Complex is composed of three unconformity-bounded stratigraphic sequences (Fig. 3). Phosphate (as francolite; $\text{Ca}_{10-a-b-c}\text{Na}_a\text{Mg}_b(\text{PO}_4)_{6-x}(\text{CO}_3)_{x-y-z}(\text{CO}_3\text{F})_y(\text{SO}_4)_z\text{F}_2$, where $x = y + a + 2c$ and $c =$ the number of Ca vacancies; Nathan, 1984) occurs throughout all three sequences, but phosphorites (beds with >10% francolite) are concentrated in the Meade Peak and Retort members of the Phosphoria Formation in the upper two

sequences. In subtidal to peritidal deposits, phosphate occurs primarily as phosphatic peloids, with phosphatic ooids, intraclasts, and phosphatized skeletal grains being less common. Phosphorites are often marked by grain-supported textures, grading, and contain mechanically abraded grains, all of which suggest mechanical reworking (McKelvey et al., 1959; Trappe, 1998; Hiatt and Budd, 2001). These attributes also suggest that these beds represent relatively shallow-water deposition.

Herein, our focus is the Meade Peak member, which is the larger of the two high-productivity deposits in the Phosphoria. Meade Peak deposition was initiated in the Late Leonardian and extended through the Roadian stage of the Guadalupian (Fig. 4). Sedimentation and phosphogenesis occurred on a nearly flat ramp with an estimated shelf depositional angle of only 0.04–0.22° between the Meade Peak depocenter and the paleoshoreline (Hiatt, 1997). The Meade Peak is a seaward-thickening wedge of sediments whose depocenter was in southeastern Idaho (Maughan, 1984). Palinspastic reconstructions and regional facies patterns in the entire Phosphoria Rock Complex have been interpreted to suggest a shelf margin just to the east of that depocenter (e.g., McKelvey et al., 1959; Peterson, 1984), but no distinctive shelf-margin facies in the Meade Peak has ever been described, which is further evidence for the ramp profile. Outer- and mid-ramp deposits include thinly bedded, finely laminated fine- to medium-grained sandstone, dolomitic siltstone, and carbonate mudstone that previous workers refer to as “shales.” Petrographic studies reveal, however, that shales are rare (Hiatt, 1997; Carroll et al., 1998). To the

east, the Meade Peak pinches out into green siltstones and carbonates, which, in turn, grade into red beds and eventually interbedded red siltstones and evaporites in central Wyoming (Fig. 4; Maughan, 1984; Peterson, 1984).

METHODS

Proxies for paleoceanographic conditions during Phosphoria Rock Complex deposition were derived from high-resolution

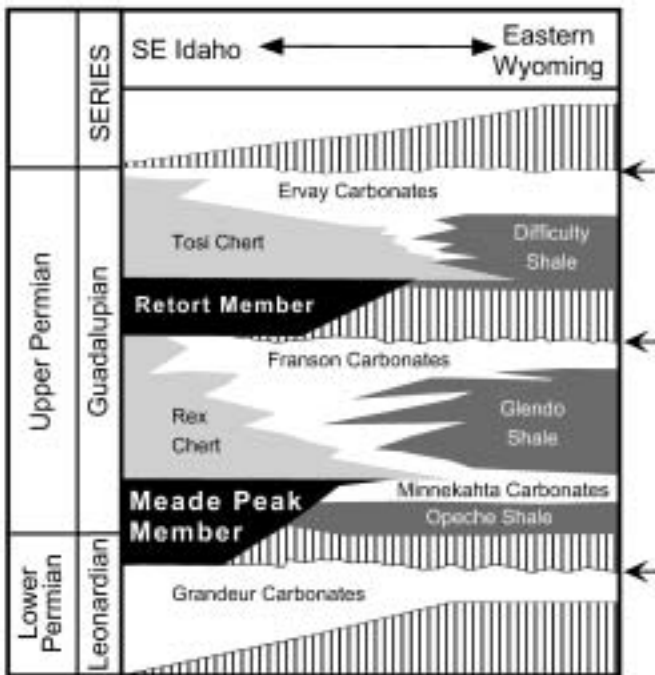


Figure 3. Stratigraphic relationships in Phosphoria Rock Complex. Vertical ruled areas denote hiatuses; arrows denote tops of unconformity-bounded sequences (modified from Maughan, 1984).

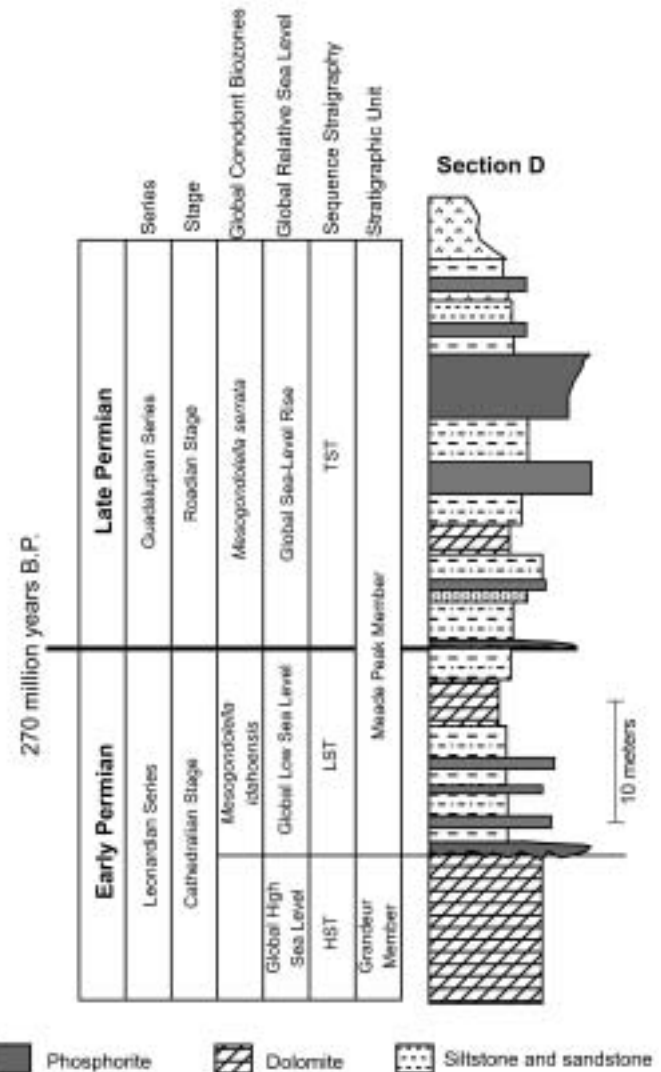


Figure 4. Generalized stratigraphic section of Meade Peak member (section D from southeastern Idaho; Fig. 5) that shows approximate position of important biostratigraphic boundary between conodonts *Mesogondolella idahoensis* and *M. serrata* (Wardlaw and Collinson, 1984), which is the accepted global boundary between Leonardian (Early Permian) and Guadalupian (Late Permian) series (Glenister et al., 1992). Series and stage names from Ross and Ross (1994). Sequence stratigraphic systems tracts from Hiatt (1997; LST—lowstand system tract, TST—transgressive system tract, HST—highstand system tract).

lithostratigraphy and chemostratigraphy. Four stratigraphic sections that form an offshore outer ramp to nearshore inner ramp transect through the Meade Peak member (Fig. 5) were utilized; they were chosen for their stratigraphic completeness and lack of visible chemical or textural alteration. Thin sections from all lithologies were examined to refine lithologic and textural classifications made during hand-sample examination. Bulk mineralogy was done by powder X-ray diffraction on a Scintag PAD-5 diffractometer. Total organic carbon (TOC) and total sulfur (TS) were determined using a Leco combustion-spectrometric device.

Phosphate grains for geochemical analyses were isolated by first disaggregating the granular phosphorite rock, sieving the resultant material into size fractions, and then passing the sand fractions through a magnetic susceptibility separator to remove glauconitic and pyritic grains. A heavy liquid separation (undiluted acetylene tetrabromide, density = 2.96 at 25 °C) was then used to remove carbonate and silicate grains. The remaining sample was washed multiple times with acetone and deionized water and dried in an oven at 80 °C for 12 hours. At this point, each size fraction was approximately 100% phosphate (francolite), as confirmed by X-ray diffraction analysis. Individual phosphatic peloids were handpicked from these concentrated and washed splits and used for the trace-element and isotopic analyses. Cadmium (Cd) concentrations were determined using X-ray fluorescence analysis; Ni and Cr concentrations were determined using instrumental neutron activation analysis. Details are given in Hiatt (1997).

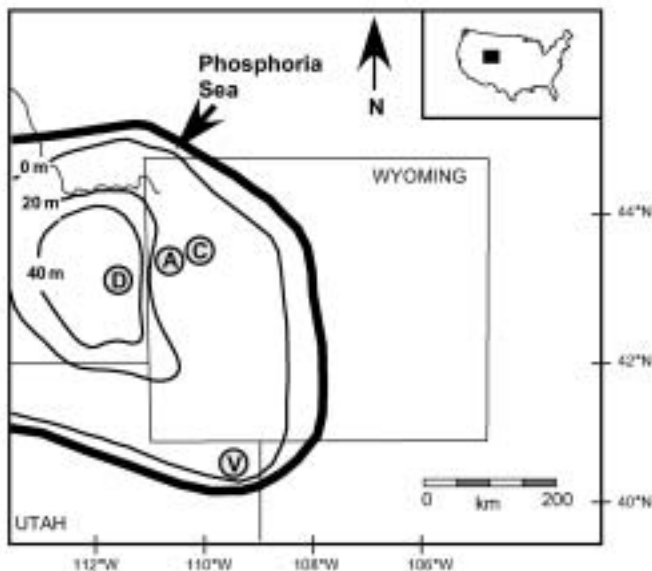


Figure 5. Map of study area showing extent of Phosphoria Sea during deposition of Meade Peak member. Isopach contours of Meade Peak member (in meters, from Maughan, 1994) and position of four stratigraphic sections utilized in this study (D—Dry Ridge; A—Astoria Hot Springs, C—Crystal Creek; V—Vernal-Brush Creek). See Hiatt (1997) for detailed locality information. Paleolatitude and base map orientation are from Scotese and Langford (1995).

Carbon isotopic values of the carbonate in the francolite crystal structure ($\delta^{13}\text{C}_{\text{PO}_4\text{-CO}_3}$) were measured in the stable isotope laboratory of the U.S. Geological Survey (USGS) in Denver. Powdered samples, averaging 100 mg in size, of isolated phosphorite peloids were reacted for 3 hours at 50 °C in individual reaction vessels with 4 ml of 100% anhydrous phosphoric acid. Evolved CO_2 was purified and isolated using two water traps maintained at -75 °C, and its isotopic composition was analyzed on a Finnigan MAT 252 mass spectrometer. Analytical precision on multiple runs ($n = 35$) of an internal calcite standard (CU-2) was ± 0.04 for $\delta^{18}\text{O}$ and ± 0.02 for $\delta^{13}\text{C}$.

All of the mineralogy, total organic carbon, total sulfur, trace element, and isotopic data generated can be found in Hiatt (1997) and is also available in tabular format from the GSA Data Repository¹. Summary tables and figures are presented herein.

RESULTS

Meade Peak Lithofacies and Biofacies

Four general lithofacies dominate the Meade Peak member in the four stratigraphic sections analyzed. These are peloidal phosphorite packstone/grainstone, peloidal phosphorite wackestone, siltstone/sandstone, and carbonate mudstone (Fig. 6). From most seaward (section D) to most landward (section V), these four sections represent outer ramp, mid ramp, inner ramp, and nearshore paleoenvironmental settings (Fig. 7).

Sediments at the Dry Ridge (52 m thick), Astoria Hot Springs (11.6 m thick) and Crystal Creek (8.1 m thick) locations (sections D, A, and C, respectively) are dark gray to black, with phosphorites comprising about 25% of each section. All the phosphorites in these sections are planar bedded; none show any visible evidence of cross bedding. Medium- to coarse-grained phosphatic peloids predominate. Intercalated with the phosphorites at Crystal Creek and Astoria Hot Springs are thin-bedded, non-fossiliferous, organic carbon-rich silty dolomite mudstones and siltstones. Intercalated facies at the Dry Ridge locality consist of bioturbated siltstone, silty carbonate mudstone, and fine- to medium-grained sandstone with hummocky cross-stratification. In contrast, in the more landward Vernal-Brush Creek section (7 m thick), all rocks are gray to tan with decimeter-thick phosphorite beds comprising 60% of the section. None of the latter phosphorites show any visible evidence of cross bedding or fining-upward textures; all are planar bedded and consist of either well-sorted fine- to medium-grained phosphatic peloids or mixtures of peloids and small intraclasts. Intercalated lithologies are thin to very thin beds of dolomitic phosphatic wackestone and silty dolomite. Further details of the sedimentology at each section are summarized by Hiatt (1997) and Hiatt and Budd (2001).

¹GSA Data Repository item 2003097, Meade Peak member samples and interpreted chemofacies, is available on request from Documents Secretary, GSA, P.O. Box 9140, Boulder, CO 80301-9140, USA, editing@geosociety.org, or at www.geosociety.org/pubs/ft2003.htm.

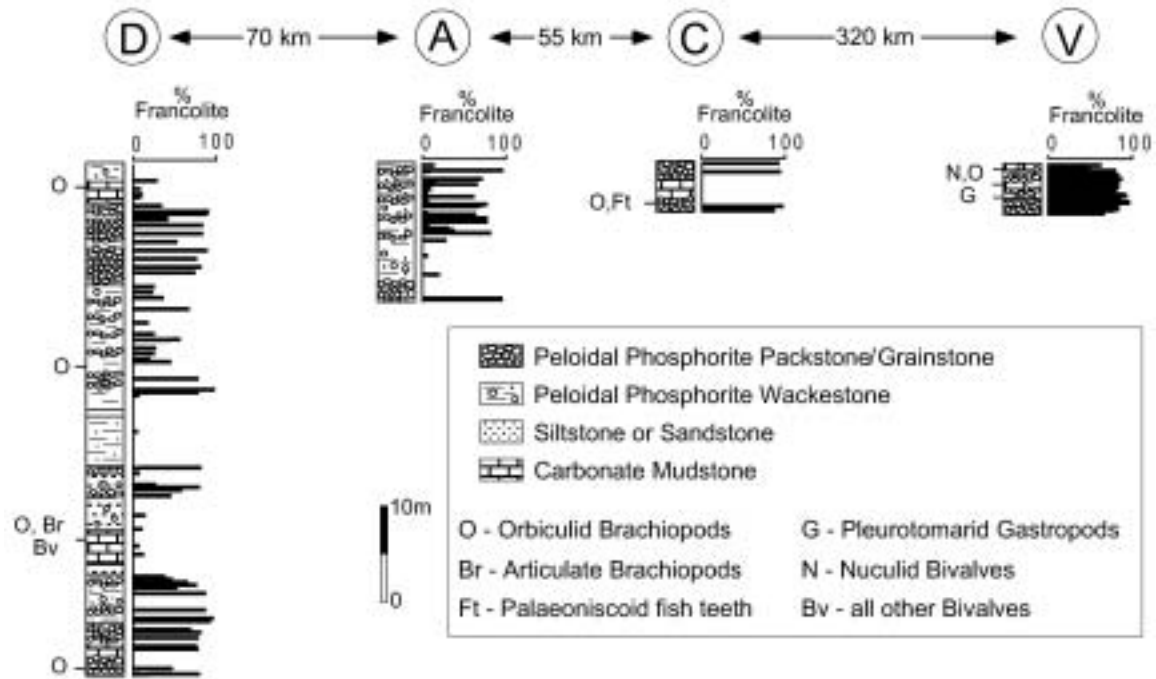


Figure 6. Stratigraphic plots of the Meade Peak member showing fauna, lithofacies, and abundance of sedimentary phosphate (as francolite).

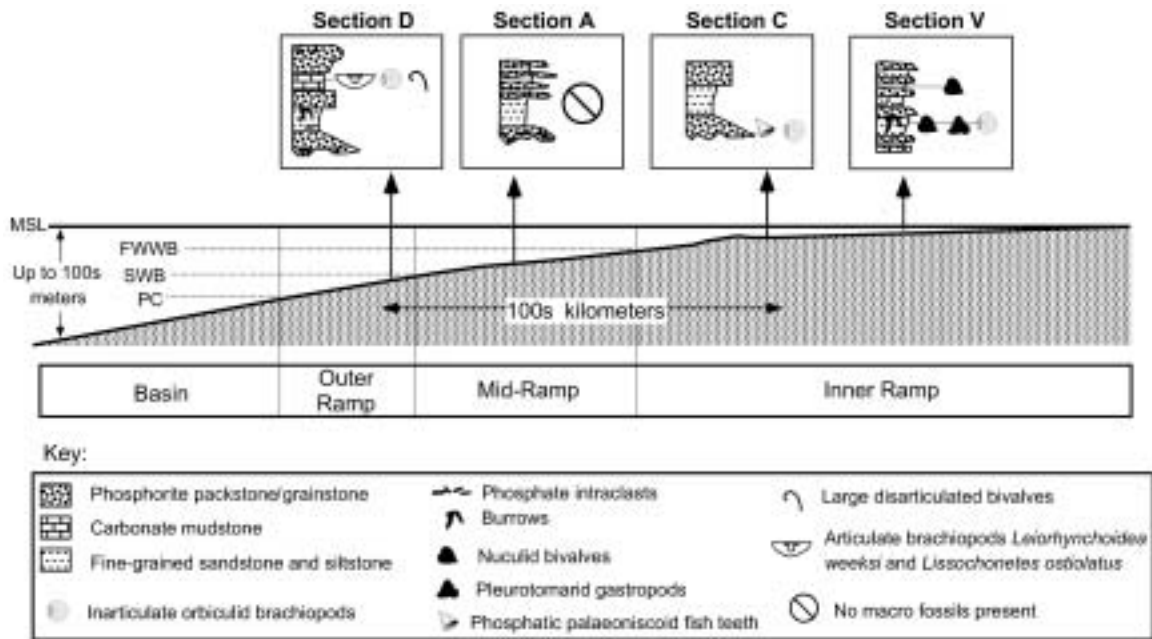


Figure 7. Diagram showing representative lithofacies associated with each Meade Peak depositional setting. See Figure 5 for section locations. Vertical exaggeration is extreme; regional slope on Wyoming paleoshelf was $<0.25^\circ$. MSL—mean sea level; FWWB—fair-weather wave base; SWB—storm wave base; PC—pycnocline.

Individual phosphorite units are not randomly distributed in the Phosphoria Rock Complex. In all four sections, phosphorite beds form the grain-rich portion of individual depositional cycles (Fig. 8). Each phosphorite usually overlies a sharp basal diastem surface. About one-fifth of those surfaces are clearly erosional as they scour into the underlying bed. Exclusive of the Vernal-Brush Creek section, about half of the phosphorites exhibit a coarse sand or pebble lag (lithoclasts up to 8 cm long) and a poorly defined fining-upward texture, which suggests deposition and winnowing in the waning phase of a high-energy storm event (cf., Föllmi, 1990). The phosphorite beds grade upward into overlying finer-grained lithofacies (siltstone, sandstone, and carbonate mudstone/wackestone) that typically contain small, in situ phosphate peloids. These finer-grained units are separated from the next phosphorite by another diastem surface (Fig. 8). The beds below the upper diastem may be bioturbated, but shelly macrofauna are not common. These relationships are consistent with Föllmi's (1990) model of alternating periods of phosphogenesis, reworking, and condensation. The basic sedimentation unit is consistent across the shelf; only the scale changes, with a general decrease in diastem-to-diastem thickness from centimeters to meters at Dry Ridge to centimeters to decimeters in the other settings.

In the outer ramp Dry Ridge section, located near the depocenter of the Meade Peak (locality D), a few beds of dolomitic mudstone contain phosphatic orbiculid inarticulate brachiopods, and the articulate brachiopods *Leiorhynchoidea weeksi* and *Lissochonetes ostiolatus*, rare benthic foraminifers, and molds of disarticulated bivalves (Figs. 6 and 7). This inarticulate and articulate brachiopod assemblage characterizes dysoxic conditions in Late Paleozoic sections worldwide (Allison et al., 1995). No macrofossils were observed in the mid ramp section (Astoria Hot Springs, section A; Figs. 6 and 7). In the inner ramp section (Crystal Creek, section C; Figs. 6 and 7), the only macrofossils observed were fish teeth (order Palaeoniscoidea) and mechanically reworked orbiculid brachiopod fragments in the lowermost phosphorite packstone/grainstone lag. A faunal assemblage consisting of orbiculid inarticulate brachiopods, phosphatized nuculoid bivalves, and pleurotomarid gastropods was found in bioturbated wackestones and abraded phosphorite lags in the nearshore section (Vernal-Brush Creek, section V; Figs. 6 and 7). These mollusks are typical of nearshore, shallow-water settings in the Late Paleozoic (Stevens, 1966).

Meade Peak Chemostratigraphy

Organic Carbon, Sulfur, and Trace Elements

The stratigraphic and regional variation of phosphate (as francolite), total organic carbon, total sulfur, Cd, and carbon isotope values from phosphate peloids ($\delta^{13}\text{C}_{\text{PO}_4\text{-CO}_3}$) for the outer-to innermost-ramp transect are shown in Figure 9 and summarized in Table 1. Sedimentary phosphate is abundant throughout the Meade Peak member. The outer ramp section (locality D) is characterized by high francolite, high total organic carbon, and some high total sulfur beds. There are also two Cd-rich intervals

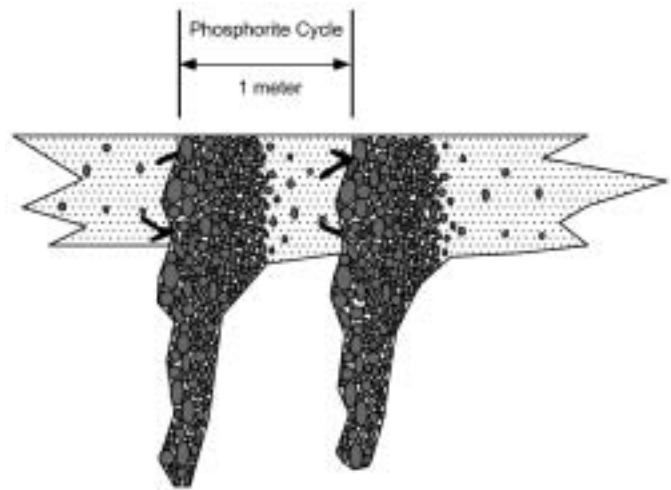


Figure 8. Generalized diagram of complete phosphorite depositional cycle in Meade Peak member of Phosphoria Rock Complex. Cycle starts with a diastem that is often erosional and bioturbated. Coarse, poorly sorted peloidal to intraclastic phosphorite is found just above diastem surface and grades into finer-grained peloidal phosphorite, followed by gradational contact with overlying organic carbon- and sulfide-rich sandstone to mudstone facies. Small, in situ phosphatic peloids are found in latter facies.

in the outer-ramp section that also exhibit high total organic carbon and high phosphate concentrations. The concurrence of these phosphate-, TOC-, and Cd-rich intervals suggests paleoproductivity peaks with low water-column oxygen levels. Throughout the mid-ramp section (locality A), there is a similar pattern of high phosphate, high total organic carbon, high total sulfur, and high Cd concentrations. Some of the highest Cd (>300 ppm), the highest total organic carbon concentrations (>10 wt%), the highest total sulfur values, and lowest TOC:TS ratios are observed in this section. The inner ramp and nearshore sections (localities C and V) are also pervasively enriched in phosphate with thin siltstone and mudstone beds separating many of the phosphorite beds in the nearshore section (too thin to be shown in Fig. 9). These two sections, however, exhibit low total organic carbon (<1 wt%) and low total sulfur (<0.4 wt%) values, and low Cd concentrations in francolite (<5 ppm).

The number of analyses of Ni and Cr is not as large as that for Cd; thus, the distribution of these elements is not shown on Figure 9, but it is summarized in Table 1. The regional trends for Ni are the same as those affecting Cd, with highest values occurring in the outer and mid-ramp sections (D and A), which are rich in organic matter. Lower values of Ni occur in the landward sections (C and V), although Ni concentrations do not decrease to the same degree abruptly as those of Cd. In contrast, Cr values are relatively high in all sections.

Carbon Isotope Data

Table 1 and Figure 9E show the stratigraphic and regional patterns of francolite $\delta^{13}\text{C}_{\text{PO}_4\text{-CO}_3}$ values in each of the four Meade Peak sections. Francolite $\delta^{13}\text{C}_{\text{PO}_4\text{-CO}_3}$ values average

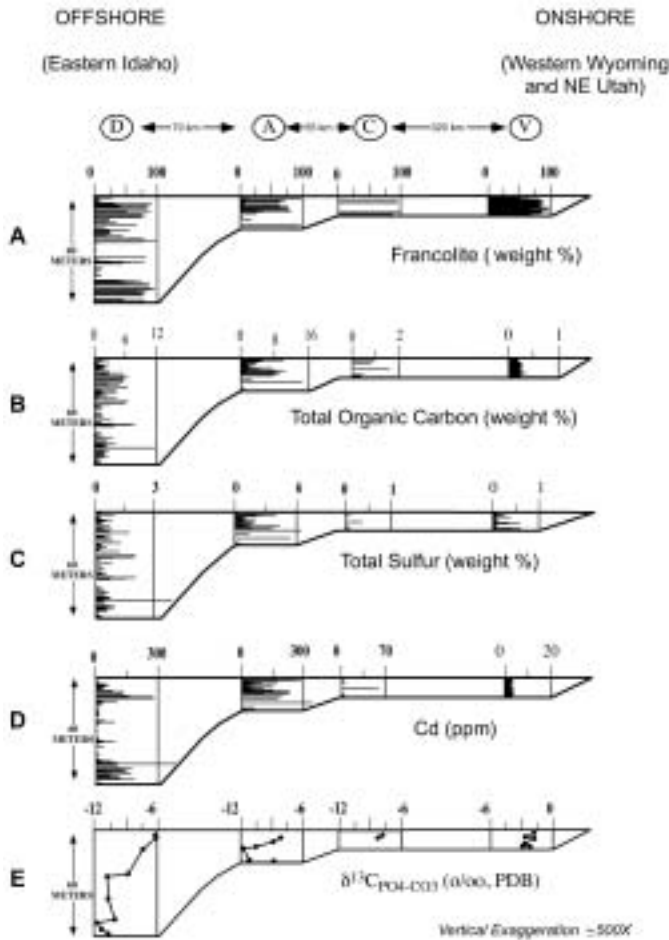


Figure 9. Regional and stratigraphic plots showing trends in (A) sedimentary phosphate (as francolite), (B) total organic carbon, (C) total sulfur, (D) Cd, and (E) $\delta^{13}\text{C}_{\text{PO}_4\text{-CO}_3}$ for Meade Peak sections in a seaward to landward transect. Francolite values are in counts per second (CPS) and are from X-ray diffraction analysis and are interpreted as semi-quantitative concentrations of francolite in rock.

$<-8.0\text{‰}$ Peedee belemnite in all but the nearshore section (locality V), where the mean is -2.7 . The most negative individual values occur in the outer and mid ramp sections (localities D and A). There is a great deal of stratigraphic variability in these two sections as well, with more negative values (nearly -12‰) near the base and a trend toward less negative values (-8 to -6‰) stratigraphically upward (Fig. 9E).

Chemofacies

A chemofacies classification was developed based on the total organic carbon content of the rocks and their total organic carbon to total sulfur ratio. These parameters have been used to estimate paleoceanographic conditions under which fine-grained siliciclastic rocks were deposited (Berner and Raiswell, 1983; Raiswell and Berner, 1986; Allison et al., 1995) and are a result

of the interplay of organic paleoproductivity, oxygen levels both in the water column and in the sediments, and in some cases, the availability of reduced iron species. This approach can present problems when used to interpret analyses of typical organic matter-bearing siliciclastics, but those shortcomings are insufficient to prevent discrimination of major geochemical facies in the Meade Peak. For example, TOC:TS ratios alone are not always able to discriminate differences in paleo-oxygen levels in organic-rich “normal marine shales” formed by typical surface productivity that have undergone significant organic burial diagenesis (Jones and Manning, 1994). However, factors such as these are not likely to generate the large, systematic, bed-by-bed differences in total organic carbon (0.1–15.7 wt%) and TOC:TS ratios (0.3–36.4) that occur in the Meade Peak (e.g., location D; Fig. 9); these are not the subtle shifts seen in “normal marine shales.” Therefore, although other methods of discriminating paleoenvironmental oxygen levels are sometimes more appropriate (e.g., degree of pyritization, Raiswell et al., 1988; indicator of anoxicity, Raiswell et al., 2001), total organic carbon values and TOC:TS ratios are sufficient to discriminate between major paleo-oceanographic differences in the Meade Peak.

Based on published total organic carbon and total sulfur values for modern and ancient environments (Berner, 1981, 1984; Berner and Raiswell, 1983; Raiswell and Berner, 1986), and allowing for diagenesis to have lowered total organic carbon values, we used these two proxies to define three broad chemofacies (Fig. 10): dysoxic, anoxic, and euxinic. The dysoxic chemofacies was simply defined as stratigraphic units with less than 1.5 wt% total organic carbon. The anoxic chemofacies occurs in beds with greater than 1.5 wt% total organic carbon and TOC:TS ratios greater than 2.0. The euxinic chemofacies is defined by total organic carbon values greater than 1.5 wt% and TOC:TS ratios less than 2.0. Figure 10A shows the range of total organic carbon and total sulfur data for all lithologies in the phosphate- and organic carbon-rich members of the Phosphoria Formation (Meade Peak data of this study plus data from the Retort member of the Phosphoria Formation; Hiatt, 1997), as well as how these values relate to published values from modern environments and to interpreted paleoenvironments. Figure 10B shows total organic carbon and total sulfur data for just the phosphorites of the Meade Peak member and the resultant chemofacies defined herein.

The average values and ranges of bulk rock total organic carbon and total sulfur values, TOC:TS ratios; Cd, Ni, and Cr concentrations; and the $\delta^{13}\text{C}_{\text{PO}_4\text{-CO}_3}$ of phosphatic peloids in each of the three chemofacies is summarized in Table 2. Combined, these data show that the dysoxic facies is characterized by low total organic carbon (by definition), low total sulfur, high TOC:TS, the least negative $\delta^{13}\text{C}_{\text{PO}_4\text{-CO}_3}$ values, and the minimum and lowest average Cd, Ni, and Cr concentrations. Of the three, only Cr has a mean concentration above 40 ppm (mean = 395 ppm) in the phosphate peloids of the dysoxic facies.

The anoxic chemofacies (Table 2) is characterized by high total organic carbon (by definition), moderate total sulfur, high TOC:TS (by definition), very negative $\delta^{13}\text{C}_{\text{PO}_4\text{-CO}_3}$, and high

TABLE 1. SUMMARY OF MEADE PEAK GEOCHEMICAL DATA BY STRATIGRAPHIC SECTION

	Section D (Dry Ridge)	Section A (Astoria Hot Springs)	Section C (Crystal Creek)	Section V (Vernal–Brush Creek)
<u>Total organic carbon</u>				
Range	0.27 to 8.50 wt	0.56 to 15.7 wt%	0.27 to 1.56 wt%	0.08 to 0.30 wt%
Average	2.63 ± 2.35	4.41 ± 3.51	0.73 ± 0.44	0.17 ± 0.05
n	79	45	6	49
<u>Total sulfur</u>				
Range	0.01 to 3.88 wt%	0.21 to 6.41 wt%	0.11 to 0.34 wt%	0.02 to 0.57 wt%
Average	0.48 ± 0.44	1.43 ± 1.39	0.21 ± 0.09	0.10 ± 0.13
n	79	45	6	49
<u>Total organic carbon:total sulfur</u>				
Range	1.8 to 36.4	0.9 to 5.6	2.0 to 7.3	0.3 to 7.3
Average	7.0 ± 5.4	3.6 ± 1.4	3.6 ± 1.9	3.4 ± 1.9
n	79	45	6	49
<u>Cd</u>				
Range	2 to 385 ppm	2 to 326 ppm	3 to 62 ppm	1 to 4 ppm
Average	51 ± 70 ppm	95 ± 78 ppm	13 ± 22 ppm	2.6 ± 0.7 ppm
n	79	45	6	49
<u>Ni</u>				
Range	40 to 540 ppm	86 to 166 ppm	40 to 115 ppm	13 to 37 ppm
Average	141 ± 169 ppm	110 ± 33 ppm	81 ± 31 ppm	21 ± 8 ppm
n	7	4	3	10
<u>Cr</u>				
Range	143 to 1540 ppm	177 to 1372 ppm	147 to 426 ppm	140 to 709 ppm
Average	430 ± 467 ppm	770 ± 460 ppm	282 ± 114 ppm	451 ± 191 ppm
n	7	4	3	10
<u>$\delta^{13}\text{C}_{\text{PO}_4\text{-CO}_3}$</u>				
Range	-11.4 to -6.0 ‰	-11.7 to -7.9 ‰	-8.1 ‰ to -7.9 ‰	-3.3 ‰ to -2.2 ‰
Average	-9.3 ± 1.9 ‰	-9.9 ± 1.3 ‰	-8.0 ± 0.1 ‰	-2.7 ± 0.3 ‰
N	11	7	2	6

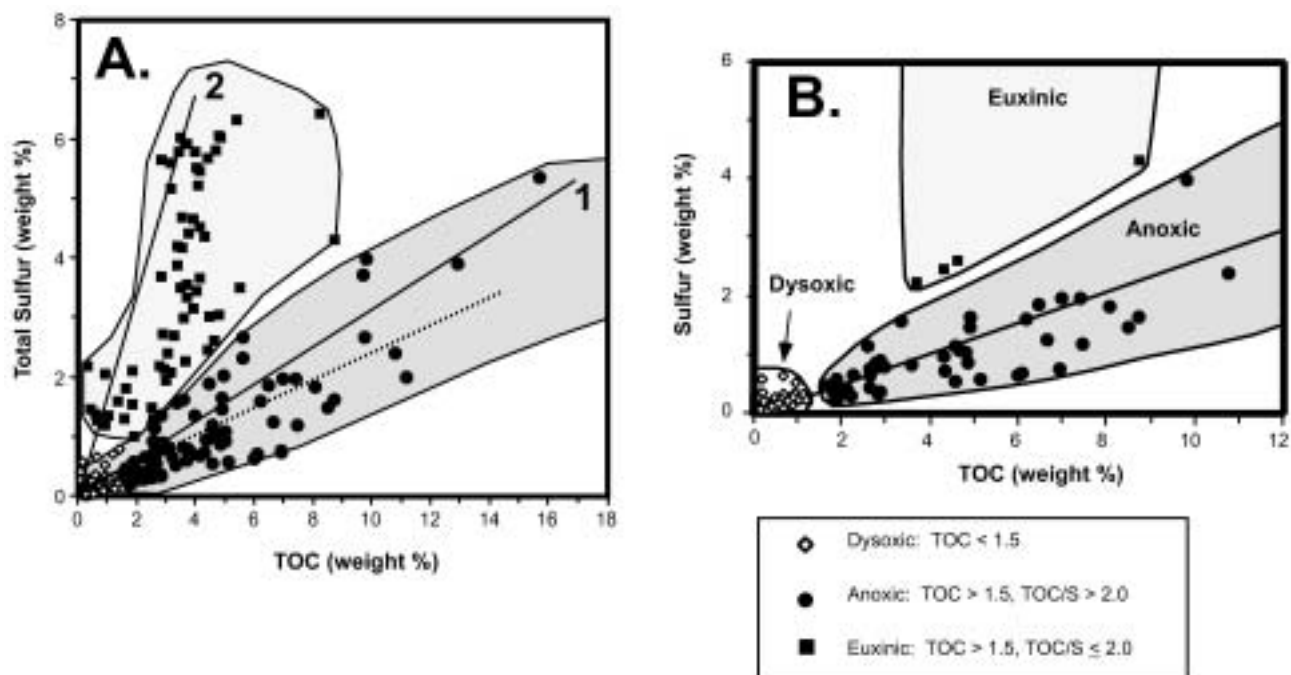


Figure 10. A: Phosphoria Rock Complex total organic carbon (TOC) and total sulfur data from all lithofacies, including non-Meade Peak rocks (additional data from Hiatt, 1997). Line 1 is trend defined by modern "normal" marine shales, and line 2 is trend for marine shales believed to have been deposited in euxinic environments (based on Berner and Raiswell, 1983). B: Total organic carbon and total sulfur data for all Meade Peak phosphorites with dysoxic, anoxic, and euxinic facies field interpretations added.

TABLE 2. SUMMARY OF MEADE PEAK GEOCHEMICAL DATA BY CHEMOFACIES

	Dysoxic chemofacies	Anoxic chemofacies	Euxinic chemofacies
<u>Total organic carbon</u>			
Range	0.08 to 1.46 wt%	1.56 to 15.7 wt%	1.66 to 8.75 wt%
Average	0.47 ± 0.40	4.82 ± 2.91	4.71 ± 3.12
n	93	81	5
<u>Total Sulfur</u>			
Range	0.01 to 0.78 wt%	0.19 to 5.35 wt%	0.99 to 6.41 wt%
Average	0.14 ± 0.05	1.03 ± 0.89	3.09 ± 1.99
n	93	81	5
<u>Total organic carbon:total sulfur</u>			
Range	0.3 to 36.4	2.1 to 9.6	0.9 to 1.9
Average	5.1 ± 5.4	5.2 ± 2.0	1.5 ± 0.4
n	93	81	5
<u>Cd</u>			
Range	1 to 181 ppm	3 to 385 ppm	16 to 218 ppm
Average	13 ± 27 ppm	85 ± 82 ppm	104 ± 84 ppm
n	93	81	5
<u>Ni</u>			
Range	13 to 115 ppm	40 to 540 ppm	86 to 98 ppm
Average	39 ± 32 ppm	144 ± 156 ppm	92 ± 6 ppm
n	14	8	2
<u>Cr</u>			
Range	140 to 709 ppm	143 to 1540 ppm	506 to 1372 ppm
Average	395 ± 192 ppm	505 ± 479 ppm	939 ± 433 ppm
n	14	8	2
<u>$\delta^{13}\text{C}_{\text{PO}_4\text{-CO}_3}$</u>			
Range	-10.1 to -2.2 ‰	-11.4 to -6.0 ‰	-11.7 ‰ to -7.9 ‰
Average	-6.6 ± 2.9 ‰	-9.8 ± 1.7 ‰	-9.8 ± 2.7 ‰
n	12	12	2

average Cd and Ni values. The euxinic chemofacies, which is the least common (n = 5), is characterized by high total organic carbon, very high total sulfur, low TOC:TS ratios (by definition), the most negative $\delta^{13}\text{C}_{\text{PO}_4\text{-CO}_3}$ values, and the highest average Cr and Cd concentrations.

Figure 11 depicts the lateral arrangement of these chemofacies and their relationship to lithofacies and macrofauna in the Meade Peak member. The sections show varying degrees of chemofacies intercalation. The one exception is the inner ramp section (locality V), which is marked exclusively by the dysoxic chemofacies. In general, the dysoxic facies dominates the nearshore Meade Peak section (locality V), whereas the anoxic chemofacies dominates both the outer ramp section and the mid ramp sections (localities D and A). The euxinic facies is found only in a few beds of the mid ramp section (Fig. 11).

DISCUSSION

Meade Peak Chemofacies and Paleoproductivity

Phosphorites are formed through chemical processes that occur independently of lithofacies. Therefore, a chemofacies approach is more indicative of the environments of phosphogenesis and a more informative paleoceanographic and paleoproductivity tool. We defined the three broad chemofacies largely on both total organic carbon values and TOC:TS ratios. The cause of high levels of organic carbon and sulfide mineral concentration and preservation has been vigorously debated. Although high concentrations of organic matter have been interpreted as simply an indicator of water column anoxia (e.g., Demaison and Moore, 1980), they are likely a complex function of biological produc-

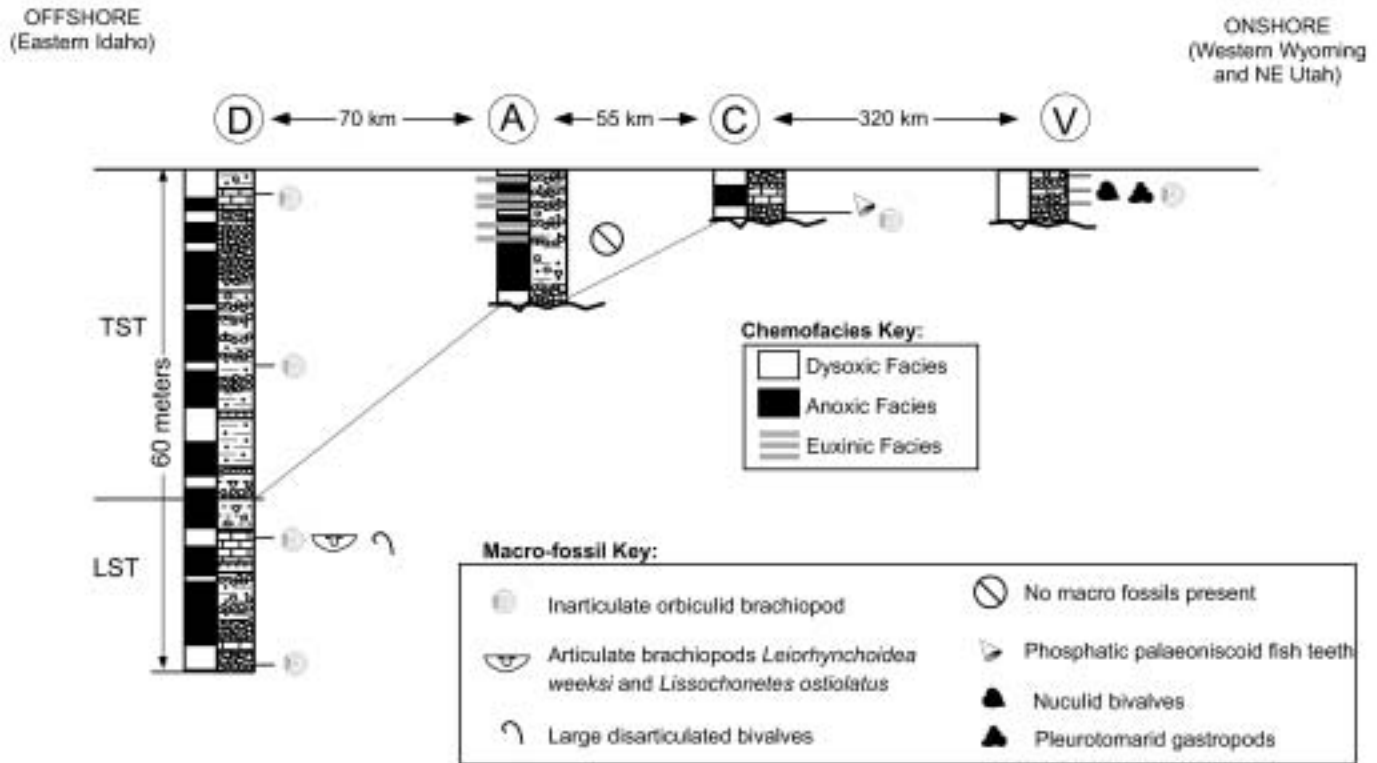


Figure 11. Meade Peak member chemofacies (left columns), lithofacies (right columns), and macrofauna (See Fig. 6 for lithofacies symbols and Fig. 5 for location information). Note that macrofossils only occur in dysoxic chemofacies. LST—lowstand systems tract; TST—transgressive systems tract.

tivity in the water column as well as sedimentation rate (e.g., Pedersen and Calvert, 1990; Canfield, 1994). Preservation of organic matter, however, is certainly enhanced under anoxic conditions (e.g., Demaison and Moore, 1980; Canfield, 1994; Ingall and Jahnke, 1997).

The important interrelationships between these factors are often lost in the debate regarding whether anoxia (e.g., Demaison and Moore, 1980) or organic productivity (e.g., Pedersen and Calvert, 1990) cause enhanced organic carbon preservation. As it falls through the water column, organic matter produced near the sea surface is broken down due to bacterial respiration (e.g., Froelich, et al., 1979; Schlesinger, 1997). Nutrients, such as phosphorus and nitrogen, are released to the water column, and oxygen is consumed in the process; if productivity is sufficient, then all water column oxygen can be consumed (e.g., Canfield, 1994). Continued breakdown of organic matter occurs after deposition leading to the release of additional phosphorus, nitrogen, and bioreactive trace elements (Froelich et al., 1979). Ingall and Jahnke (1997) pointed out that these processes are particularly important where upwelling-induced marine productivity occurs, because once nutrients are added (P, N, and sometimes Fe), increased biological productivity can quickly result in consumption of all oxygen in the water column below. Ingall and Jahnke showed that a positive feedback can develop, in which breakdown of organic matter leads to anoxic conditions that, in turn,

increase phosphorus regeneration and enhance organic matter preservation. The regenerated phosphorus is released to the intra-sediment porewater, where it can be fixed as sedimentary phosphate (francolite), and to the water column, where it contributes to further enhancement of productivity (Ingall and Jahnke, 1997).

Concentrations of Cd, Ni, and Cr in the phosphatic peloids augment the chemofacies approach because these elements are known to exhibit nutrient-like distributions in the modern oceans (e.g., Broecker and Peng, 1982; Calvert and Pedersen, 1993; Nathan et al., 1997; Schlesinger, 1997) and are concentrated in sediments under low-oxygen conditions (e.g., Calvert and Pedersen, 1993). Furthermore, Cd, and possibly Ni, is fixed as sulfides in sediments under sulfate reducing conditions, but Cr becomes concentrated in sediments under the less-reducing conditions of denitrification (Piper, 2001). In sediments and sedimentary rocks, these elements can be used to track past nutrient levels and paleoceanographic conditions because they are incorporated into the preserved sediments, whereas the actual nutrients (e.g., P and N) are largely recycled and remobilized in the depositional environment. These elements have been linked to biological processes and are characteristic of sediments deposited in highly productive oceanic areas today (e.g., Broecker and Peng, 1982; Schlesinger, 1997). In particular, phytoplankton concentrate Cd, and although concentrations are high, Piper et al. (2000) showed that Cd/Zn ratios in the Meade Peak member are similar to those

found in modern plankton. With subsequent bacterial breakdown of organic matter, Cd can become highly concentrated in the organic residue (Gauthier et al., 1986). Ni, a micro-nutrient to many organisms, is associated with high marine productivity, and it promotes the growth of anaerobic bacteria (Cox, 1995).

The low total organic carbon and total sulfur values and low Cd, Ni, and Cr concentrations of the dysoxic Meade Peak chemofacies are all compatible with the presence of O₂ in the depositional environment and, thus, compatible with the recycling rather than burial of organic-carbon and nutrients. The low concentrations of the nutrient proxies (Cd, Ni, and Cr) suggest either low nutrient levels and/or aerobic conditions. We believe the latter to be the appropriate interpretation, because Cr exhibits a relatively high mean concentration (395 ppm). Unlike the other trace-element proxies for nutrients, Cr has multiple oxidation states and can be concentrated in sediments associated with high productivity under dysoxic conditions (Murray et al., 1983; Calvert and Pedersen, 1993). The fact that Cr concentrations in the phosphatic peloids of the dysoxic facies are not as low as the concentrations of the other trace elements suggests that nutrients were not limited, just effectively recycled by bacterial respiration of organic matter under denitrifying conditions (Piper, 2001). The oxygen present in the water, however, prevented sulfate reduction either in the water column or in the sediment that would have formed sulfide and trapped Cd and Ni, making their concentrations generally low.

In contrast, the high total organic carbon, high TOC:TS, and high average Cd and Ni values of the Meade Peak anoxic facies is compatible with an absence of O₂ in the water column and sediments. Free hydrogen sulfide in the water column must also have been absent; otherwise, total sulfur values would be higher and TOC:TS values would not be as great.

The very high concentrations of Cd in the anoxic chemofacies are probably indicative of high nutrient levels and a greater flux of organic matter to the seafloor. In the modern ocean, Cd concentrations are highest where sulfide is present in the sediment because it is incorporated into iron sulfide phases (Van Geen et al., 1994). The lack of covariance, however, between Cd and total sulfur (Fig. 9) indicates that Cd concentrations are not linked directly to pyrite content, but Cd is instead high because of extreme surface productivity and was incorporated into the francolite crystal structure under low oxygen conditions (cf., Nathan et al., 1997). The absence of O₂ suggested by this chemofacies points to ineffective recycling of organic matter and nutrients, thus the high total organic carbon values in the sediments and high trace-element concentrations in the francolite. However, the fact that such conditions persisted and dominated the outer and mid ramp settings (Fig. 11) means that the nutrient influx to these settings must have been maintained; otherwise, nutrients would have become limited, and paleoproductivity would have slowed or ceased. This, in turn, suggests that the anoxic chemofacies marks the sites of intense and persistent upwelling.

Finally, the high total organic carbon, very high total sulfur, and low TOC:TS values, and high Cd and Cr concentrations of

the euxinic Meade Peak chemofacies are all compatible with an absence of O₂ and the presence of free hydrogen sulfide in the water column and sediments. Total organic carbon levels are similar to those of anoxic facies (Table 1), indicating that high productivity prevailed in the water column, coupled with effective preservation. Extremely high pyrite concentrations suggest that iron was readily available and was probably sourced from terrigenous clastic sediments supplied by wind (cf. Carroll et al., 1998) or as shown for euxinic conditions in the Black Sea (Canfield et al., 1996), from breakdown of particulate organic matter in the water column. Hypereutrophic, sulfate-reducing conditions probably existed, and productivity was restricted to phytoplankton. Indeed, biomarker studies (Dahl et al., 1993; and Stephens and Carroll, 1999) indicate that phytoplankton and bacteria were abundant in the water column over the mid-ramp euxinic chemofacies. The average trace element concentrations are much higher than the dysoxic facies, and thus are compatible with high nutrient levels and reducing conditions. As with the anoxic facies, the euxinic chemofacies must also mark the site of intense and persistent upwelling.

The intercalation of anoxic and dysoxic chemofacies in the outer and inner ramp settings (Fig. 11) does suggest either temporal and/or spatial shifts in upwelling intensity away from the mid-ramp locus of upwelling and paleoproductivity. Movement in time and space of upwelling farther onto the paleoramp would generate changes in the location of maximum surface productivity and thus cause a switch from anoxic to dysoxic in the outer ramp and a concurrent switch from dysoxic to anoxic in the inner ramp. The converse, movement off the paleoramp, would generate the opposite effects in both settings. Assuming depositional rates measured in millimeters per 1000 yr or less, the thickness of the intercalated chemofacies (centimeters to meters) indicates a forcing factor with a frequency measured in 10⁵ or more years. What such factors might have been is unclear to us, although fluctuations in global ocean circulation patterns are certainly feasible. A link between extreme paleoproductivity and southern-hemisphere glaciation has been suggested by prior workers (e.g., Pardee, 1917; Sheldon, 1984; Piper and Kolodny, 1987), and glacio-eustasy has also been implied in the interpretation of cyclicity in other Phosphoria Rock Complex units (e.g., Hendrix and Byers, 2000; Trappe, 2000). However, a glacio-eustatic climate and/or sea-level driver must be considered unlikely, given that recent biostratigraphic constraints establish that widespread glaciation in Gondwanaland ended millions of years before deposition of the Meade Peak phosphate and organic, carbon-rich units (Fig. 2).

Carbon Isotopic Variation

In general, the primary $\delta^{13}\text{C}_{\text{PO}_4\text{-CO}_3}$ values of phosphorites represent a largely benthic signal derived as francolite forms and recrystallizes due to microbial-mediated reactions within centimeters of the sediment-water interface (e.g., Jarvis, 1992; Jarvis et al., 1994). Burial diagenesis can lower $\delta^{13}\text{C}_{\text{PO}_4\text{-CO}_3}$

values; the Phosphoria phosphorites are widely perceived to represent an advanced diagenetic end member (McArthur et al., 1986; Jarvis et al., 1994). Interpretation of the Meade Peak $\delta^{13}\text{C}_{\text{PO}_4\text{-CO}_3}$ data thus requires that we first evaluate the possibility of burial alteration.

The burial alteration hypothesis, as articulated by McArthur et al. (1986) and Jarvis et al. (1994) assumes that Miocene and younger phosphorites define the primary isotopic composition of francolites regardless of geologic age. Implicit in this assumption is the idea that all sedimentary francolites have formed under similar environmental conditions, which ignores secular changes in ocean-water chemistry and the diverse paleoenvironmental settings in which ancient phosphorites are known to have formed (e.g., Cook et al., 1990; Glenn et al., 1994). In fact, it is becoming clear that the Meade Peak phosphorites did not form under environmental conditions like any Neogene or Quaternary phosphogenic environment (Dahl et al., 1993; Hiatt, 1997; Stephens and Carroll, 1999; Hiatt and Budd, 2001; Piper and Link, 2002). Thus, the diagenetically unaltered young phosphorites are not reasonable analogs for the initial $\delta^{13}\text{C}_{\text{PO}_4\text{-CO}_3}$ of the Meade Peak phosphorites.

The burial alteration hypothesis also ignores the fact that some geochemical proxies are much less likely to alter than others. Shemesh et al. (1988) concluded that $\delta^{18}\text{O}_{\text{PO}_4\text{-CO}_3}$ (isotopic value isolated from the structural carbonate site within the francolite crystal lattice) values were altered in many phosphorites, but that $\delta^{13}\text{C}_{\text{PO}_4\text{-CO}_3}$ and $\delta^{18}\text{O}_{\text{PO}_4}$ (isotopic value isolated from the structural phosphate site within the francolite crystal lattice) values were extremely resistant to diagenetic alteration. Because modern and ancient phosphorites show ranges of similar magnitude in their carbon isotopic values, the $\delta^{13}\text{C}_{\text{PO}_4\text{-CO}_3}$ values in francolite may be better preserved over geologic time than the simple burial alteration hypothesis presumes (Shemesh et al., 1988; Kolodny and Luz, 1992).

The Meade Peak $\delta^{13}\text{C}_{\text{PO}_4\text{-CO}_3}$ values reported herein do show some covariance with burial depth. The most negative values occur in the outer ramp section (Fig. 9E), which experienced the greatest burial depths (5.5 km, Hiatt and Budd, 2001). The least negative values occur in the nearshore section (Fig. 9E), which experienced the least burial depths (3 km, Hiatt and Budd, 2001). A least-square linear regression between $\delta^{13}\text{C}_{\text{PO}_4\text{-CO}_3}$ values and the maximum burial depth of the four localities yields an *R*-value of 0.69. However, this apparent covariance may just be a coincidence, as the deepest buried sections (D and A) are also the most organic-rich sections. A linear regression between $\delta^{13}\text{C}_{\text{PO}_4\text{-CO}_3}$ and total organic carbon in the same rock samples yields an *R*-value of 0.66, which is statistically indistinguishable from the value derived from the regression against maximum burial depth. The $\delta^{13}\text{C}_{\text{PO}_4\text{-CO}_3}$ of the Meade Peak phosphorites is thus just as likely to be a function of the total organic carbon of the rock as it is to be one of burial alteration. Of course, total organic carbon values have probably also been reduced by organic diagenesis; however, the analysis of chemofacies suggests that the main control on total organic carbon variation is

changes in paleoproductivity. By analogy, we thus conclude that the primary depositional conditions across the ramp are also recorded in the $\delta^{13}\text{C}_{\text{PO}_4\text{-CO}_3}$ signal, although some diagenetic alteration cannot be completely ruled out.

As a proxy of primary depositional conditions across the Meade Peak ramp, the interpretation of the $\delta^{13}\text{C}_{\text{PO}_4\text{-CO}_3}$ values must include consideration of the chemofacies. The least negative $\delta^{13}\text{C}_{\text{PO}_4\text{-CO}_3}$ values reflect the least influence of organic ^{12}C . Such values occur in the dysoxic facies (Table 2), which is compatible with the more complete recycling of organic matter before burial below the sediment-water interface. As the francolite formed below that interface, it thus did not incorporate as much organic ^{12}C as francolite formed in the other chemofacies. The anoxic and euxinic facies would represent the opposite situation. High burial rates of organic matter due to inefficient recycling in the water column would have meant pore waters enriched in organic ^{12}C , and thus the more negative $\delta^{13}\text{C}_{\text{PO}_4\text{-CO}_3}$ values for the francolites formed in those chemofacies (Table 2). Indeed, McArthur et al. (1986) predicted that the carbon isotopic signature of francolite precipitated in dysoxic porewater should have a $\delta^{13}\text{C}_{\text{PO}_4\text{-CO}_3}$ value of -2% to -6% , and those precipitated in anoxic porewater should have $\delta^{13}\text{C}_{\text{PO}_4\text{-CO}_3}$ values of -6% to -15% (PDB). These ranges are similar to those observed in the Meade Peak phosphorites (Tables 1 and 2). The lateral and vertical variations in $\delta^{13}\text{C}_{\text{PO}_4\text{-CO}_3}$ values (Fig. 9E) are thus further evidence that the process of phosphogenesis in the Meade Peak occurred across a broad spatial and temporal range of paleoceanographic conditions.

Phosphogenesis in the Phosphoria Sea

In mid and outer ramp settings where total organic carbon and total sulfur values, nutrient trace-element proxies, and phosphorite percentages are all high, phosphogenesis likely occurred much as it does in the modern ocean, albeit in much shallower waters. That is, large amounts of organic matter accumulated on the seafloor where primary productivity was extreme. Anoxic conditions within the sediments and bacterial breakdown of the organic matter (Froelich et al., 1979) released organic-bound phosphorous into the sediments (Filippelli and Delaney, 1996; Ingall and Jahnke, 1997). This process lead to phosphogenesis, while attendant anoxic conditions led to high amounts of sulfide and organic matter, and the efficient “trapping” of the nutrient-like cations in the sediments (Westerlund et al., 1986; Nathan et al., 1997). Continued influx of upwelled waters provided a source of new nutrients; thus, high productivity, high burial rates of organic carbon, and phosphogenic processes can be long lasting.

Conditions on the inner ramp appear to have been much different. Abundant phosphorite yet low total organic carbon and total sulfur values and low nutrient-like trace-element concentrations indicate that phosphogenesis in the shallow nearshore environments must have either differed in some way from that described above, or all nearshore phosphorites were derived by long distance transport from mid-ramp settings. Although some

of those nearshore phosphorites may be allochthonous, others clearly are not. In particular, the presence of small, phosphatized peloids in the intercalated carbonate muds is suggestive of in situ phosphogenesis in this setting. The phosphatization of the infaunal bivalves, many of which are still articulated and in their original burrows (Hiatt and Budd, 2001), also argues for autochthonous phosphogenesis on the inner ramp. A variation on the standard phosphogenesis model is thus needed to account for the phosphorites of the inner ramp setting.

The abundance of nearshore phosphorite formation indicates that there must have been a significant influx of phosphorous, which in turn means an influx of nutrient-rich waters to the innermost part of the ramp. Although riverine inputs have been documented for some nearshore phosphorites (e.g., Föllmi, 1996), we do not consider that a likely source for the Meade Peak phosphorites. The adjacent coastal landmass was characterized by evaporite deposits (Maughan, 1984; Peterson, 1984), and there is no published evidence for fluvial inputs to the Phosphoria Sea during Meade Peak deposition. A major source of detrital material to the sediments that make up the Meade Peak was derived by eolian influx (Carroll et al., 1998). Thus, the only viable source of nutrients was the water that upwelled farther seaward in the area of maximum upwelling (mid-ramp position) and eventually flowed into the inner ramp.

Ingall and Jahnke (1997) showed that phosphorus is more efficiently regenerated to the water column relative to organic matter under anoxic conditions. The corollary to this scenario is that where organic matter breaks down in dysoxic settings, such as the inner ramp, phosphorus is more likely to be fixed as francolite at the same time organic matter is consumed (Van Cappellen and Ingall, 1994). Therefore, phosphorus released to waters flowing from the anoxic environments in the mid-ramp could have fed productivity in the inner ramp. Oxygen supplied by air-sea exchange in these shallow-water settings, however, seems to have prevented the seawater, seafloor, and sediments from becoming anoxic, which in turn suppressed sulfide formation. Organic matter must have been efficiently recycled at and just below the sediment-water interface, resulting in low preserved total organic carbon. Over time, a net flux of phosphorous into phosphorites would occur, but because of the winnowing effect of storm-generated waves and the addition of oxygen through exchange with the atmosphere, there would be little preservation of organic carbon. Reasonably high productivity, coupled with high water temperatures on the inner ramp (Hiatt and Budd, 2001), may have resulted in a stable, possibly thermally (Piper and Link, 2002) or salinity (Dahl et al., 1993; Stephens and Carroll, 1999) stratified dysoxic water column that limited benthic dissolved oxygen levels and was supplied with enough nutrients to maintain phosphogenesis. Phosphogenesis in such a setting is distinctly different than any modern environment of phosphogenesis.

The low Cd and Ni concentrations of the inner ramp phosphorites also imply efficient recycling of these nutrient-like cations, and/or their depletion in the nearshore organic matter and

the presence of oxygen in the water. Depletion is plausible if a significant percentage of the mass of these cations that was brought onto the Phosphoria ramp with upwelling waters was "trapped" in the anoxic outer- and mid-ramp sediment as sulfides. Anoxic marine basins are known to efficiently trap Cd and other metals in their sediments (Westerlund et al., 1986). Because of the superb textural preservation of all Meade Peak phosphorites, and the fact that the highest cation concentrations are found in the most deeply buried sections (localities D and A), we do not believe the low Cd, Ni, and Cr concentrations of the inner-ramp phosphorites are due to diagenetic mobilization.

Reassessment of the Paleocology of the Phosphoria Rock Complex Biota

It has long been noted that the faunas of the Phosphoria and equivalent rocks exhibit low faunal diversity and abundance relative to age-equivalent lower-latitude sections (Yochelson, 1968; Wardlaw and Collinson, 1984; Boyd, 1993). Yochelson (1968), in the most comprehensive study of Phosphoria Rock Complex paleontology, interpreted this low diversity to be the result of low water temperatures. Wardlaw (1980) and Wardlaw et al. (1995) furthered the general acceptance of a cold-water "Arctic" fauna. The only dissenting voice to date has been that of Peterson (1980, 1984), who noted that maximum faunal diversity in the Phosphoria Rock Complex occurred in the carbonate bioherms of the Rex Chert member (Fig. 3) near the western border of Wyoming, where upwelling is predicted to have been most intense. As a result, Peterson reasoned that cool water was unlikely to have caused the low faunal diversity in the Phosphoria Rock Complex because diversity was apparently greatest where the water would have been the coldest.

We concur with Peterson (1980, 1984) that cool water was not the major biolimiting agent in the Meade Peak member and probably in the entire Phosphoria Rock Complex. Instead, the data described herein shows that macrofossils in the Meade Peak member occur almost exclusively in beds of the dysoxic chemofacies (Fig. 11). Bioturbation, described in detail by Hendrix and Byers (2000), is probably also limited to beds that would fall into our dysoxic chemofacies category. The anoxic chemofacies rarely contains macrofossils, and when present, the macrofossils always show signs of mechanical reworking. The euxinic chemofacies never contains any macrofauna or bioturbation. Where the latter two chemofacies prevailed, seafloor oxygen levels must have been so low as to exclude even the low diversity dysaerobic communities that characterize portions of the dysoxic facies.

Elevated salinity levels and possible salinity stratification caused by brines flowing westward from evaporative basins to the east of the Phosphoria Sea (Hite, 1978, Dahl et al., 1993; Stephens and Carroll, 1999) could also be a factor in explaining the faunal distribution, but Piper and Link (2002) determined that the Phosphoria Sea was probably temperature-stratified, not salinity-stratified. The absence of macrofauna in the highly productive mid-ramp section (Fig. 7A), where upwelling and influx

of normal salinity ocean water from the west would have been greatest, further suggests that salinity was not the major biolimiting agent. Our data clearly suggest that the low faunal diversity and abundance of the Meade Peak member is related first and foremost to low oxygen levels.

Although we believe oxygen levels to be the foremost biolimiting factor in the Meade Peak, temperature probably did play a role. However, that role was primarily related to warm temperatures, not cold. This is evidenced by a comparison of the macrofauna in the dysoxic outer ramp facies (section D) with the macrofauna in the most landward sections (section V). Hiatt and Budd (2001) showed the outer ramp section was the site of cool, but not cold, paleotemperatures. As noted previously, the macrofauna in that section is composed of small chonetid and leiorhynchid articulate brachiopods, a few small bivalves, and orbiculid inarticulate brachiopods. This is the only Meade Peak member assemblage that closely approximates a “normal,” albeit dysoxic Late Paleozoic marine fauna (Allison et al., 1995). In contrast, the faunal assemblage of the inner ramp and nearshore sections consists only of orbiculid inarticulate brachiopods, nuculoid bivalves, and pleurotomarid gastropods (Figs. 6 and 13), which is indicative of restricted shallow water, dysaerobic conditions of variable salinity (Stevens, 1966; Kammer et al., 1986). Restriction, shallow water, and the broad nature of the ramp setting all resulted in mean paleotemperatures in excess of 30 °C (Hiatt and Budd, 2001), which may have raised salinities due to evaporation and limited the biota. In this setting, oxygen levels are the primary control on the fauna, but warm temperature is a secondary factor due to the lower solubility of oxygen at higher water temperatures and the greater consumption of oxygen by bacterial respiration.

The argument for oxygen as the dominant biolimiting factor in the paleoecology of the Meade Peak is also strengthened by a critical reanalysis of the arguments for an “Arctic” fauna. In particular, the cold water “Arctic” fauna interpretation, which is based on ammonites and one species each of conodont and brachiopod (Wardlaw, 1980; Wardlaw et al., 1995), is weakened when the distribution of all Phosphoria Rock Complex fauna is considered in the context of recent plate tectonic reconstructions.

The conodont *Mesogondolella phosphoriensis* (= *Mesogondolella rosenkrantzi*; Wardlaw et al., 1995) is cited as one line of evidence for an “Arctic” fauna (Wardlaw, 1980). However, other reported occurrences of *M. phosphoriensis* are at paleolatitude less than or equal to 40° when plotted on the modern plate reconstruction of Scotese and Langford (1995). Specifically, the data of Bender and Stoppel (1965), Toulou (1875), Sweet (1976), and Szaniawski and Malkowski (1979) indicate that this conodont is found at Permian paleolatitudes of 27°N (Greenland), 3°S (Sicily), and 40°N (Spitsbergen). This suggests that *M. phosphoriensis* may not be indicative of an “Arctic” fauna after all. Further, it has been reported only in the upper meter or so of the Meade Peak member (Wardlaw and Collinson, 1984), yet four other conodont species are found throughout the Meade Peak that are also widespread in low-latitude, Paleotethys and equatorial

sections of western North America (e.g., *Mesogondolella serrata*, *M. gracilis*, *M. idahoensis*, and *Neostreptognathodus sulcificatus*; Yugan et al., 1994; Behnken et al., 1986; Igo, 1981; Szaniawski and Malkowski, 1979). The presence of these widespread “warm”-water conodonts in the Meade Peak member is not easily explained in the context of an “Arctic” fauna.

The case for a “cool water brachiopod fauna” in the Phosphoria Rock Complex (Wardlaw, 1980) is based on the presence of *Neospirifer striato-paradoxus*, which was originally described by Toulou (1875) from Spitzbergen (Permian paleolatitude of 40°N). Specimens of *N. striato-paradoxus* were identified in the Phosphoria Rock Complex in rocks of Middle Wordian age (Wardlaw, 1980), which constrains the stratigraphic unit to either the Franson or the Rex Chert member of the Park City Formation (Fig. 4). Thus, this “Arctic” form is not found in the stratigraphic units associated with maximum paleoproductivity (the Meade Peak and Retort members) as has often been assumed (Parrish, 1982; Parrish and Peterson, 1988; Whelan, 1993; Inden and Coalson, 1996).

There are also several Phosphoria Rock Complex brachiopods that are characteristic of low-latitude North American and Paleotethys locations. These include *Kuvelousia leptosa*, which is common in the equatorial Paleotethys region and is found in the Rex Chert and Franson members of the Phosphoria Rock Complex in southwestern Montana (Wardlaw, 1977). There is also extensive overlap between the Phosphoria Rock Complex brachiopod fauna and sections near the paleo-equator of west Texas (Yochelson, 1968; Brittenham, 1973), Mexico (Wardlaw et al., 1979), and south China (Xu and Grant, 1994). As with the conodonts, the entire brachiopod fauna does not present a convincing argument for cold water.

Lastly, support for the “cool-water” model was also deduced from ammonoids. Wardlaw et al. (1995; p. 36) pointed out that specimens of the ammonoid genus *Daubichites* found in the Meade Peak member have “...been reported (Spinosa and Nassichuk, 1985) as having a ‘boreal’ or cool-water, high-latitude distribution.” However, Spinosa and Nassichuk (1985) also pointed out that *Daubichites* is a geographically widespread ammonoid and, in addition to its occurrence in the Meade Peak member, it is also found in the equatorial Paleotethys (Siberia, Australia, China) and northern Canada. More recently, an equatorial Permian ammonoid (*Demarezites furnishi*) was reported from the Meade Peak of southeastern Idaho (Spinosa and Nassichuk, 1994); the only other reported occurrences of this ammonoid are from west Texas and central Mexico (Spinosa and Nassichuk, 1994), areas that were situated within 10° of the Permian equator.

In summary, Phosphoria Rock Complex conodont, ammonite, and brachiopod faunas have some affinities to high-latitude Permian settings but do not provide a convincing and overwhelming argument for widespread and persistent “cool-water” conditions in the Phosphoria Sea. There are, in fact, just as many similarities in the fauna assemblage to warm, tropical settings. This suggests that other environmental factors served as the primary biolimiting

agent. The chemofacies distributions defined herein clearly indicate that oxygen availability was more likely the cause of a sparse Phosphoria Rock Complex fauna in general and Meade Peak fauna in particular.

NEW PALEOCEANOGRAPHIC MODEL FOR THE PHOSPHORIA UPWELLING SYSTEM

Information from Recent Climate Models

Findings from climate models for the Permian are relevant to any reinterpretation of phosphogenesis and paleoceanography in the Phosphoria Rock Complex. Kutzbach and Ziegler (1994) produced a high-resolution model that included inland seas, large lakes, and marine embayments like the Phosphoria Sea. Their model indicates that the atmosphere over the Phosphoria Sea would have had a mean annual surface air temperature of 30–35 °C with summer surface air temperatures rising as high as 45 °C. These temperatures are in agreement with paleotemperatures of phosphogenesis in the inner ramp setting determined by Hiatt and Budd (2001). East-to-west eolian transport is also predicted from modeled wind directions, which is compatible with an eolian source for the Meade Peak siltstones and sandstones (Carroll et al., 1998). The modeled temperature and rainfall results also agree with geological evidence that indicates an extremely hot desert surrounding the Phosphoria Sea (Sheldon et al., 1967; Ziegler, 1990). Kutzbach and Ziegler's (1994) model thus seems to be geologically reasonable.

Kutzbach and Ziegler's (1994) climate model also shows a drastic wintertime weakening of the atmospheric circulation system and thus attendant reduction in coastal upwelling in the Phosphoria Sea (Fig. 1). The possibility that upwelling was seasonal is particularly important. Surface waters during summer upwelling and phosphogenesis would have been subject to hot (35–45 °C) air temperatures and would have become very warm in the shallow inner ramp. In the winter, the cessation of coastal upwelling would have meant that the waters in the Phosphoria Sea became restricted, possibly stratified, and extreme warming could have occurred in nearshore settings.

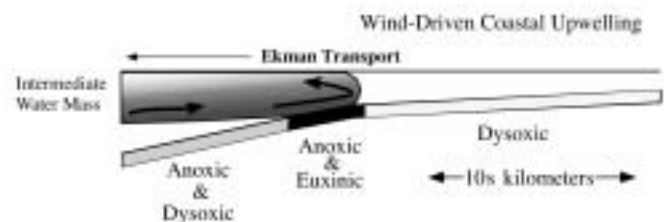
The New Paleocceanographic Model

New research and our improved understanding of the modern ocean indicate that the modern Peru-margin analog traditionally used to explain the Phosphoria upwelling system needs to be reassessed. That model cannot account for the variety of paleoenvironments that led to phosphogenesis or the relationship between paleoproductivity and macrofauna distribution. A new paleoceanographic model for the Phosphoria upwelling system is necessary.

The new paleoceanographic model that we propose (Fig. 12) takes into account the shallow and broad ramp setting, warm paleotemperatures (Hiatt and Budd, 2001), seasonal upwelling predicted by climate models (Kutzbach and Ziegler, 1994), severe oxygen depletion, high nutrient levels, and the new

geochemical data presented herein. In this interpretation, oxygen-depleted, nutrient-rich water impinged on the Wyoming paleoramp at the mid-ramp position, where anoxia and euxinic conditions prevailed (present-day western Wyoming). Given the semi-restricted, shallow, marginal nature of the Phosphoria Sea, it is unlikely that an open-ocean deep-water mass could have been accessed by the wind-driven upwelling system. The more probable source of this nutrient-rich, oxygen-depleted water was a northward-flowing intermediate water mass (Jewell, 1995). Indeed, nutrient-rich, oxygen-poor water is near the surface over large areas between 20° N and 20° S today (Levitus, 1982), and a much more extreme oxygen-depleted, warm, nutrient-rich intermediate water mass is predicted for the west coast of equatorial Pangea during the Permian (Jewell, 1995; Hotinski et al., 2001). This intermediate layer probably extended into the Phosphoria Sea and was brought to the surface during the summertime, when wind patterns produced coastal upwelling by Ekman transport (Fig. 12). Upwelling may have ceased in winter, which allowed the waters, especially in the inner-ramp setting, to warm and approximate the overlying air temperatures.

A. Summer (Mean Air Temperatures 35–45 °C)



B. Winter (Mean Air Temperatures 25–30 °C)

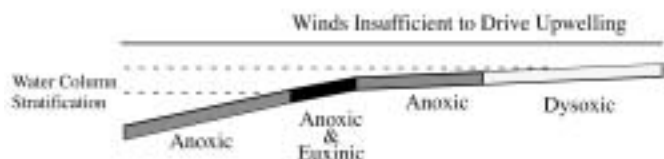


Figure 12. Conceptual model showing distribution of chemofacies, upwelling, and seasonal variation within Phosphoria Sea during Meade Peak deposition. A: Summertime case in which an oxygen-depleted, nutrient-rich water mass enters Phosphoria Sea and is driven to surface and seaward by coastal upwelling. High biological productivity in mid-ramp caused high organic particulate flux to seafloor, where bacterial respiration consumed all dissolved oxygen. Regeneration of phosphorus provided a supply of nutrients to inner ramp setting, where phosphogenesis occurred under dysoxic conditions. B: Wintertime case in which wind strength decreased and direction changed (Kutzbach and Ziegler, 1994) such that it was not able to maintain significant upwelling. Possible thermal stagnation may have occurred, water temperature of inner to mid-ramp settings would have risen, and continued bacterial respiration of organic matter in water column and below sediment-water interface would have consumed oxygen and resulted in expansion of anoxic and euxinic conditions.

The water flowing into the Phosphoria embayment probably had little or no dissolved oxygen to begin with, but as it warmed, its oxygen-carrying capacity remained extremely low, which prevented significant oxygen uptake from the atmosphere. This, combined with bacterial respiration of organic matter in the water column, favored development of widespread anoxia and even euxinic conditions. Even in nearshore environments, oxygen uptake would have been limited, and the water never became more than dysaerobic. As a result, macrofauna were suppressed due to low oxygen stress while phosphogenesis occurred in environments that ranged from dysoxic shallow inner-ramp settings to predominately anoxic mid- and outer-ramp settings. Salinity variation between the inner ramp and outer ramp probably influenced which organisms lived in which of those two settings, but the complete absence of macrofossils in the mid ramp suggests that elevated salinity did not play a major role in controlling the presence/absence of macro organisms in any setting. Paleoproductivity indicators suggest that maximum upwelling occurred in the mid-ramp position, and thus there was an ample influx of ocean water that would have prevented the elevation of salinity at this location.

This new model and our findings have great significance for the interpretation of other ancient phosphorites and suggest that paleoceanographic setting and paleoenvironment must be taken into account to fully understand the geochemical variation seen in ancient phosphorites.

CONCLUSIONS

The late Early to Late Permian is an important transitional time in earth history; the Phosphoria Rock Complex spans this change in global oceanographic, climatic, and biotic regimes. The widespread continental glaciation that marked the southern continents during the Early Permian had ended long before the phosphorites of the Phosphoria Rock Complex began forming. Extreme oceanographic conditions marked the Phosphoria Sea, and sedimentary phosphate and organic carbon were deposited across a broad range of paleoceanographic and paleoenvironmental settings, a range of phosphogenetic environments not seen today. Specifically:

1. Phosphogenesis in the Phosphoria Rock Complex occurred in depositional environments ranging from "basinal" outer ramp settings in <200 m water depth to very shallow, restricted inner ramp environments.

2. The organic carbon, sulfur, trace element, and $\delta^{13}\text{C}_{\text{PO}_4\text{-CO}_3}$ signatures vary systematically with position on the shelf, reflecting diverse paleoceanographic conditions across the paleoshelf and phosphogenesis in dysoxic to euxinic conditions.

3. Phosphogenesis in anoxic settings is strongly related to paleoproductivity indicators and occurred much as it does in the modern ocean, albeit in much shallower waters. Large amounts of organic matter accumulated on the seafloor due to the anoxic conditions and breakdown of the organic-matter-released, organic-bound phosphorous that in turn led to phosphogenesis.

4. Abundant phosphorite, yet low total organic carbon and total sulfur values and low, nutrient-like, trace-element concentrations indicate that phosphogenesis in nearshore, shallow-water, dysoxic settings was dramatically different. Oxygen supplied by air-sea exchange in these shallow-water settings maintained low oxygen levels and promoted the recycling of organic matter from the sediments. Yet, some of the liberated phosphorous produced phosphorites. Reasonably high productivity coupled with high water temperatures resulted in a stable dysoxic water column that was supplied with just enough nutrients to maintain phosphogenesis.

5. Cations that serve as paleoproductivity indicators are in low concentrations in the nearshore dysoxic settings due to either their efficient recycling or their "trapping" in the anoxic outer- and mid-ramp sediment.

6. Based on integration of lithofacies, biofacies, and chemofacies it is clear that the traditional cold- and deep-water upwelling model for the Meade Peak is not tenable. A more realistic paleoceanographic model is one in which a northward-flowing, oxygen-depleted, nutrient-rich intermediate water mass impinged on the seafloor at the mid-ramp position where anoxic and euxinic conditions prevailed. This shallow intermediate layer extended into the Phosphoria Sea and was brought to the surface during the summertime, when wind patterns produced coastal upwelling by Ekman transport. The water probably had very little dissolved oxygen to begin with, and as it warmed in the shallow waters of the Phosphoria Sea, its oxygen-carrying capacity remained extremely low. As a result, the upwelled water mass never became more than dysaerobic in nearshore environments, yet it was still capable of driving phosphogenesis in shallow-water settings.

7. Macrofauna in the Meade Peak member are only found in dysoxic facies, and their absence elsewhere (anoxic and euxinic chemofacies) is related first and foremost to low oxygen levels. Macrofauna also exhibit lateral variations that can be related to warm temperatures on the paleo ramp, but these variations are secondary to the control exerted by oxygen levels. All prior workers who use the occurrence, distribution, and nature of the Phosphoria Rock Complex fauna to argue for a simple cold-water upwelling model failed to recognize this point.

ACKNOWLEDGMENTS

We thank the donors of the Petroleum Research Fund, administered by the American Chemical Society, for financial support. Additional support was provided to EEH by Texaco, the Colorado Scientific Society, Exxon, and an American Association of Petroleum Geologists student grant. We thank Noel James, Josef Werne, Peir Pufahl, and Laura Gates for thoughtful reviews that improved the final version of this manuscript. Robert Rye kindly provided access to the U.S. Geological Survey stable isotope laboratory, Fred Luizer (University of Colorado) performed the X-ray fluorescence analyses and Halina Szymczyk (Texaco) provided the total organic carbon and total sulfur analyses.

REFERENCES CITED

- Allison, P.A., Wignall, P.B., and Brett, C.E., 1995, Palaeo-oxygenation: Effects and recognition, *in* Bosence, D.W.J., and Allison, P.A., eds., Marine palaeoenvironmental analysis from fossils: Geological Society [London] Special Publication 83, p. 97–112.
- Barron, E.J., and Fawcett, P.J., 1995, The climate of Pangea: A review of climate model simulations of the Permian, *in* Scholle, P.A., Peryt, T.M., and Ulmer-Scholle, D.S., eds., The Permian of northern Pangea, Volume 1: Paleogeography, paleoclimates, stratigraphy: Berlin, Springer-Verlag, p. 37–52.
- Behnken, F.H., Wardlaw, B.R., and Stout, L.N., 1986, Conodont biostratigraphy of the Permian Meade Peak Phosphatic Shale member, Phosphoria Formation, southeastern Idaho: Laramie, Wyoming, University of Wyoming, Contributions to Geology, v. 24, p. 169–190.
- Bender, V.H., and Stoppel, D., 1965, Perm-Conodonten: Geologisches Jahrbuch, v. 82, p. 331–364.
- Berner, R.A., 1981, A new geochemical classification of sedimentary environments: Journal of Sedimentary Petrology, v. 51, p. 359–365.
- Berner, R.A., 1984, Sedimentary pyrite formation: An update: Geochimica et Cosmochimica Acta, v. 48, p. 605–615.
- Berner, R.A., 1994, GEOCARB II: a revised model of atmospheric CO₂ over Phanerozoic time: American Journal of Science, v. 294, p. 56–91.
- Berner, R.A., and Raiswell, R., 1983, Burial of organic carbon and pyrite sulfur in sediments over Phanerozoic time: A new theory: Geochimica et Cosmochimica Acta, v. 47, p. 855–862.
- Boyd, D.W., 1993, Paleozoic history of Wyoming, *in* Steidtmann, J.R., and Roberts, S.M., eds., Geology of Wyoming, Volume 1: Geological Society of Wyoming Memoir 5, p. 164–187.
- Brittenham, M.D., 1973, Permian Phosphoria bioherms and related facies, southeastern Idaho [Master's thesis]: Missoula, University of Montana, 213 p.
- Broecker, W.S., and Peng, T.-H., 1982, Tracers in the sea: Palisades, New York, Eldigio Press, Lamont-Doherty Geological Observatory, 690 p.
- Calvert, S.E., and Pedersen, T.F., 1993, Geochemistry of Recent oxic and anoxic marine sediments: Implications for the geological record: Marine Geology, v. 113, p. 67–88.
- Canfield, D.E., 1994, Factors influencing organic carbon preservation in marine sediments: Chemical Geology, v. 114, p. 315–329.
- Canfield, D.E., Lyons, T.W., and Raiswell, R., 1996, A model for iron deposition to euxinic Black Sea sediments: American Journal of Science, v. 296, p. 818–834.
- Carroll, A.R., Stephens, N.P., Hendrix, M.S., and Glenn, C.R., 1998, Eolian-derived siltstone in the Upper Permian Phosphoria Formation: Implications for marine upwelling: Geology, v. 26, p. 1023–1026.
- Cathcart, J.B., Sheldon, R.P., and Gulbrandsen, R.A., 1984, Phosphate-rock resources of the United States: U.S. Geological Survey Circular 888, 48 p.
- Claypool, G.E., Love, A.H., and Maughan, E.K., 1978, Organic geochemistry, incipient metamorphism, and oil generation in black shale members of Phosphoria Formation, western interior United States: American Association of Petroleum Geologists Bulletin, v. 62, p. 98–120.
- Cook, P.J., and McElhinny, M.W., 1979, A reevaluation of the spatial and temporal distribution of sedimentary phosphate deposits in the light of plate tectonics: Economic Geology, v. 74, p. 315–330.
- Cook, P.J., Shergold, J.H., Burnett, W.C., and Riggs, S.R., 1990, Phosphorite research: A historical overview, *in* Notholt, A.J.G., and Jarvis, I., eds., Phosphorite research and development: Geological Society [London] Special Publication 52, p. 1–22.
- Cox, P.A., 1995, The elements on Earth: Oxford, Oxford University Press, 287 p.
- Dahl, J., Moldovan, J.M., and Sundaraman, P., 1993, Relationship of biomarker distribution to depositional environment: Phosphoria Formation, Montana, U.S.A.: Organic Geochemistry, v. 20, p. 1001–1017.
- Demaison, G.J., and Moore, G.T., 1980, Anoxic environments and oil source bed genesis: American Association of Petroleum Geologists Bulletin, v. 64, p. 1179–1209.
- Dickins, J.M., 1984, Late Palaeozoic glaciation: B.M.R. Journal of Australian Geology and Geophysics, v. 9, p. 163–169.
- Dickins, J.M., 1996, Problems of a Late Palaeozoic glaciation in Australia and subsequent climate in the Permian: Palaeogeography, Palaeoclimatology, Palaeoecology, v. 125, p. 185–197.
- Filippelli, G.M., and Delaney, M.L., 1996, Phosphorus geochemistry of equatorial Pacific sediments: Geochimica et Cosmochimica Acta, v. 60, p. 1479–1495.
- Föllmi, K.B., 1990, Condensation and phosphogenesis: Example of the Helvetic mid-Cretaceous (northern Tethyan margin), *in* Notholt, A.J.G., and Jarvis, I., eds., Phosphorite research and development: Geological Society [London] Special Publication 52, p. 237–252.
- Föllmi, K.B., 1996, The phosphorus cycle, phosphogenesis and marine phosphate-rich deposits: Earth Science Reviews, v. 40, p. 55–124.
- Frakes, L.A., Francis, J.E., and Syktus, J.I., 1992, Climate modes of the Phanerozoic: Cambridge, Cambridge University Press, 274 p.
- Froelich, P.N., Klinkhammer, G.P., Bender, M.L., Luedtke, N.A., Heath, G.R., Cullen, D., Dauphin, P., Hammond, D., Hartman, B., and Maynard, V., 1979, Early oxidation of organic matter in pelagic sediments of the eastern equatorial Atlantic—Suboxic diagenesis: Geochimica et Cosmochimica Acta, v. 43, p. 1075–1090.
- Gauthier, M.J., Clément, R.L., Flatau, G.N., and Amiard, J.-C., 1986, Accumulation du cadmium par les bactéries marines à Gram négatif selon leur sensibilité au métal et leur type respiratoire: Oceanologica Acta, v. 9, p. 333–337.
- Glenister, B.F., Boyd, D.W., Furnish, W.M., Grant, R.E., Harris, M.T., Kozur, H., Lambert, L.L., Nassichuk, W.M., Newell, N.D., Pray, L.C., Spinosa, C., Wardlaw, B.R., Wilde, G.L., and Yancey, T.E., 1992, The Guadalupian: Proposed international standard for a Middle Permian Series: International Geology Review, v. 34, p. 857–888.
- Glenn, C.R., Föllmi, K.B., Riggs, S.R., Baturin, G.N., Grimm, K.A., Trappe, J., Abed, A.M., Galli-Olivier, C., Garrison, R.E., Ilyin, A.V., Jehl, C., Rohrlisch, V., Sadaqah, R.M.Y., Schidlowski, M., Sheldon, R.P., and Siegmund, H., 1994, Phosphorus and phosphorites: Sedimentology and environments of formation: Eclogae Geologicae Helveticae, v. 87, p. 747–788.
- González-Bonorino, G., and Eyles, N., 1995, Inverse relation between ice extent and the Late Paleozoic glacial record of Gondwana: Geology, v. 23, p. 1015–1018.
- Hendrix, M.S., and Byers, C.W., 2000, Stratigraphy and sedimentology of Permian strata, Unita Mountains, Utah: Allostratigraphic controls on the accumulation of economic phosphate, *in* Glenn, C.R., Lucas, J., and Lucas, J., eds., Marine authigenesis: From global to microbial: SEPM (Society for Sedimentary Geology) Special Publication 66, p. 349–367.
- Hiatt, E.E., 1997, A paleoceanographic model for oceanic upwelling in a Late Paleozoic epicontinental sea: A chemostratigraphic analysis of the Permian Phosphoria Formation [Ph.D. thesis]: Boulder, University of Colorado, 294 p.
- Hiatt, E.E., and Budd, D.A., 2001, Sedimentary phosphate formation in warm shallow waters: New insights into the paleoceanography of the Permian Phosphoria Sea from analysis of phosphate oxygen isotopes: Sedimentary Geology, v. 145, p. 119–133.
- Hite, R.J., 1978, Possible genetic relationships between evaporites, phosphorites, and iron-rich sediments: The Mountain Geologist, v. 14, p. 97–107.
- Hotinski, R.M., Bice, K.L., Kump, L.R., Najjar, R.G., and Arthur, M.A., 2001, Ocean stagnation and end-Permian anoxia: Geology, v. 29, p. 7–10.
- Igo, H., 1981, Permian conodont biostratigraphy of Japan: Palaeontological Society of Japan Special Paper 24, p. 1–50.
- Inden, R.F., and Coalson, E.B., 1996, Phosphoria Formation (Permian) cycles in the Bighorn Basin, Wyoming, with emphasis on the Ervay member, *in* Longman, M.W., and Sonnenfeld, M.D., eds., Paleozoic systems of the Rocky Mountain region: Denver, The Rocky Mountain Section of SEPM (Society for Sedimentary Geology), p. 379–404.
- Ingall, E., and Jahnke, R., 1997, Influence of water-column anoxia on the elemental fractionation of carbon and phosphorus during sediment diagenesis: Marine Geology, v. 139, p. 219–229.
- Jarvis, I., 1992, Sedimentology, geochemistry and origin of phosphatic chalks: The Upper Cretaceous deposits of NW Europe: Sedimentology, v. 39, p. 55–97.
- Jarvis, I., Burnett, W.C., Nathan, Y., Almbaydin, F.S.M., Attia, A.K.M., Castro, L.N., Flicoteaux, R., Hilmy, M.E., Husain, V., Qutawnah, A.A., Serjani, A.,

- and Zanin, Y.N., 1994, Phosphorite geochemistry: State-of-the-art and environmental concerns: *Eclogae Geologicae Helveticae*, v. 87, p. 643–700.
- Jewell, P.W., 1995, Geologic consequences of globe-encircling equatorial currents: *Geology*, v. 23, p. 117–120.
- Jones, B., and Manning, D.A.C., 1994, Comparison of geochemical indices used for the interpretation of palaeoredox conditions in ancient mudstones: *Chemical Geology*, v. 111, p. 111–129.
- Kammer, T.W., Brett, C.E., Boardman, D.R.I., and Mapes, R.H., 1986, Ecologic stability of the dysaerobic biofacies during the Late Paleozoic: *Lethaia*, v. 19, p. 109–121.
- Ketner, K.B., 1977, Late Paleozoic orogeny and sedimentation, southern California, Nevada, Idaho, and Montana, in Stewart, J.H., Stevens, C.H., and Fritsche, A.E., eds., *Paleozoic paleogeography of the western United States, Pacific Coast Paleogeography Symposium 1: Los Angeles, The Pacific Section of Society of Economic Paleontologists and Mineralogists*, p. 363–369.
- Kolodny, Y., and Luz, B., 1992, Isotope signatures in phosphate deposits: Formation and diagenetic history, in Clauer, N., and Chaudhuri, S., eds., *Isotopic signatures and sedimentary records: Berlin, Springer-Verlag*, p. 69–121.
- Knoll, A.H., Bambach, R.K., Canfield, D.E., and Grotzinger, J.P., 1995, Comparative earth history and Late Permian mass extinction: *Science*, v. 273, p. 452–457.
- Kutzbach, J.E., and Ziegler, A.M., 1994, Simulation of Late Permian climate and biomes with an atmosphere-ocean model: Comparisons with observations, in Allen, J.R.L., Hoskins, B.J., Sellwood, B.W., Spicer, R.A., and Valdes, P.J., eds., *Palaeoclimates and their modeling: London, Chapman and Hall*, p. 119–132.
- Levitus, S., 1982, *Climatological atlas of the world ocean: National Oceanic and Atmospheric Administration Professional Paper 13*, p. 173.
- Maughan, E.K., 1984, Geological setting and some geochemistry of petroleum source rocks in the Permian Phosphoria Formation, in Woodward, J., Meissner, F.F., and Clayton, J.L., eds., *Hydrocarbon source rocks of the Greater Rocky Mountain region: Denver, Rocky Mountain Association of Geologists*, p. 281–294.
- Maughan, E.K., 1994, Phosphoria Formation (Permian) and its resource significance in the Western Interior, U.S.A, in Embry, A.F., Beauchamp, B., and Glass, D.J., eds., *Pangea: Global environments and resources: Calgary, Canadian Society of Petroleum Geologists Memoir 17*, p. 479–495.
- McArthur, J.M., Benmore, R.A., Coleman, M.L., Soldi, C., Yeh, H.-W., and O'Brien, G.W., 1986, Stable isotope characterisation of francolite formation: *Earth and Planetary Science Letters*, v. 77, p. 20–34.
- McKelvey, V.E., Cheney, T.M., Cressman, E.R., Sheldon, R.P., Swanson, R.W., and Williams, J.S., 1959, The Phosphoria, Park City, and Shedhorn formations in the western phosphate field: *U.S. Geological Survey Professional Paper 313-A*, 47 p.
- McKelvey, V.E., Swanson, R.W., and Sheldon, R.P., 1953, The Permian phosphorite deposits of western United States, in Saint Guilhem, M.R., ed., *Origine des gisements de phosphates de chaux: 19th International Geological Congress (1952), Comptes rendus, sec. 11, no. 11, Algiers*, p. 45–64.
- Murray, J.W., Spell, B., and Paul, B., 1983, The contrasting geochemistry of manganese and chromium in the eastern tropical Pacific Ocean, in Wong, C.S., Boyle, E., Bruland, K.W., Burton, J.D., and Goldberg, E.D., eds., *Trace metals in sea water: New York, Plenum Press*, p. 643–669.
- Nathan, Y., 1984, The mineralogy and geochemistry of phosphorites, in Nriagu, J.O., and Moore, P.B., eds., *Phosphate minerals: Heidelberg, Springer-Verlag*, p. 275–291.
- Nathan, Y., Soudry, D., Levy, Y., Shitrit, D., and Dorfman, E., 1997, Geochemistry of cadmium in the Negev phosphorites: *Chemical Geology*, v. 142, p. 87–107.
- Pardee, J.T., 1917, The Garrison and Philipsburg phosphate fields, Montana: *U.S. Geological Survey Bulletin 640*, p. 195–228.
- Parrish, J.T., 1982, Upwelling and petroleum source beds, with reference to the Paleozoic: *American Association of Petroleum Geologists Bulletin*, v. 66, p. 750–774.
- Parrish, J.T., and Peterson, F., 1988, Wind directions predicted from global circulation models and wind directions determined from eolian sandstones of the western United States—A comparison: *Sedimentary Geology*, v. 56, p. 261–282.
- Pedersen, T.F., and Calvert, S.E., 1990, Anoxia vs. productivity: What controls the formation of organic-carbon-rich sediments and sedimentary rocks?: *American Association of Petroleum Geologists Bulletin*, v. 74, p. 454–466.
- Peterson, J.A., 1980, Depositional history and petroleum geology of the Permian Phosphoria, Park City, and Shedhorn formations, Wyoming and southeastern Idaho: *U.S. Geological Survey Open File Report 80-667*, p. 42.
- Peterson, J.A., 1984, Permian stratigraphy, sedimentary facies, and petroleum geology, Wyoming and adjacent area, in Goolsby, J., and Morton, D., eds., *The Permian and Pennsylvanian geology of Wyoming: Wyoming Geological Association, Guidebook 35*, p. 25–64.
- Piper, D.Z., 2001, Marine chemistry of the Permian Phosphoria Formation and basin, southeast Idaho: *Economic Geology*, v. 96, p. 599–620.
- Piper, D.Z., and Kolodny, Y., 1987, The stable isotopic composition of a phosphorite deposit: $\delta^{13}\text{C}$, $\delta^{34}\text{S}$, and $\delta^{18}\text{O}$: *Deep-Sea Research*, v. 34, p. 897–911.
- Piper, D.Z., and Link, P.K., 2002, An upwelling model for the Phosphoria sea: A Permian, ocean-margin sea in the northwest United States: *American Association of Petroleum Geologists Bulletin*, v. 86, p. 1217–1235.
- Piper, D.Z., Skorupa, J.P., Presser, T.S., Hardy, M.A., Hamilton, S.J., Huebner, M., and Gulbrandsen, R.A., 2000, The Phosphoria Formation at the Hot Springs Mine in Southeast Idaho: A source of selenium and other trace elements to surface water, ground water, vegetation, and biota: *U.S. Geological Survey Open-File Report 00-050*, 73 p.
- Raiswell, R., and Berner, R.A., 1986, Pyrite and organic matter in Phanerozoic normal shales: *Geochimica et Cosmochimica Acta*, v. 50, p. 1967–1976.
- Raiswell, R., Buckley, F., Berner, R.A., and Anderson, T.F., 1988, Degree of pyritization of iron as a paleoenvironmental indicator of bottom-water oxygenation: *Journal of Sedimentary Petrology*, v. 58, p. 812–819.
- Raiswell, R., Newton, R., and Wignall, P.B., 2001, An indicator of water-column anoxia: Resolution of biofacies variation in the Kimmeridge Clay (Upper Jurassic, U.K.): *Journal of Sedimentary Research*, v. 71, p. 286–294.
- Rees, P.M., Gibbs, M.T., Ziegler, A.M., Kutzbach, J.E., Behling, P.J., 1999, Permian climates: Evaluating model predictions using global paleobotanical data: *Geology*, v. 27, p. 891–894.
- Ross, C.A., and Ross, J.R.P., 1994, Permian sequence stratigraphy and fossil zonation, in Embry, A.F., Beauchamp, B., and Glass, D.J., eds., *Pangea: Global environments and resources: Canadian Society of Petroleum Geologists Memoir 17*, p. 219–231.
- Schlesinger, W.H., 1997, *Biogeochemistry: San Diego, Academic Press*, 588 p.
- Scotese, C.R., and Langford, R.P., 1995, Pangea and the paleogeography of the Permian, in Scholle, P.A., Peryt, T.M., and Ulmer-Scholle, D.S., eds., *The Permian of northern Pangea. Volume 1: Paleogeography, paleoclimates, stratigraphy: Berlin, Springer-Verlag*, p. 3–19.
- Sheldon, R.P., 1963, Physical stratigraphy and mineral resources of Permian rocks in western Wyoming: *U.S. Geological Survey Professional Paper 313-B*, 273 p.
- Sheldon, R.P., 1984, Polar glacial control on sedimentation of Permian phosphorites of the Rocky Mountains, USA: *Proceedings of the 27th International Geological Congress, Moscow: Utrecht, The Netherlands, VNU Science Press*, v. 15, p. 223–243.
- Sheldon, R.P., 1989, Phosphorite deposits of the Phosphoria Formation, Western United States, in Notholt, A.J.G., Sheldon, R.P., and Davidson, D.F., eds., *Phosphate deposits of the world: Volume 2, phosphate rock resources: Cambridge, Cambridge University Press*, p. 53–61.
- Sheldon, R.P., Maughan, E.K., and Cressman, E.R., 1967, Sedimentation of rocks of Leonard (Permian) age in Wyoming and adjacent states, in Hale, L.A., ed., *Anatomy of the western phosphate field: Salt Lake City, Utah, 15th Annual Field Conference, Intermountain Association of Geologists*, p. 1–13.
- Skipp, B., and Hall, W.E., 1980, Upper Paleozoic paleotectonics and paleogeography of Idaho, in Fouch, T.D., and Magathan, E.R., eds., *Paleozoic paleogeography of the west-central United States: Rocky Mountain Paleogeography Symposium 1: Denver, Rocky Mountain Section of Society of Economic Paleontologists and Mineralogists*, p. 387–419.

- Shemesh, A., Kolodny, Y., and Luz, B., 1988, Isotopic geochemistry of oxygen and carbon in phosphate and carbonate of phosphorite francolite: *Geochimica et Cosmochimica Acta*, v. 52, p. 2565–2572.
- Spinosa, C., and Nassichuk, W.W., 1985, The Permian ammonoid *Uraloceras* in North America and its global significance: *Geological Society of America Abstracts with Programs*, v. 17, p. 724.
- Spinosa, C., and Nassichuk, W.W., 1994, The Permian ammonoid *Demareziites ruzhencevi* from the Phosphoria Formation, Idaho: *Journal of Paleontology*, v. 68, p. 1036–1040.
- Stephens, N.P. and Carroll, A.R., 1999, Salinity stratification in the Permian Phosphoria Sea: A proposed paleoceanographic model, *Geology*, v. 27, p. 899–902.
- Stevens, C.H., 1966, Paleoecologic implications of Early Permian fossil communities in eastern Nevada and western Utah: *Geological Society of America Bulletin*, v. 77, p. 1121–1130.
- Sweet, W.C., 1976, Conodonts from the Permian-Triassic boundary beds at Kap Stosch, East Greenland, in Teichert, C., and Kummel, B., eds., *Permian-Triassic boundary in the Kap Stosch area, East Greenland: Meddelelser Om Gronland*, v. 197, no. 5, p. 51–54.
- Szaniawski, H., and Malkowski, K., 1979, Conodonts from the Kapp Starostin Formation (Permian) of Spitsbergen: *Acta Palaeontologica Polonica*, v. 24, p. 231–264.
- Taylor, E.L., Taylor, T.N., and Cúneo, N.R., 1992, The present is not the key to the past: A polar forest from the Permian of Antarctica: *Science*, v. 257, p. 1675–1677.
- Toula, F., 1875, *Permo-Carbon-Fossilien von der Westkuste von Spitzbergen: Neues Jahrbuch fur Mineralogie, Geologie und Palaontologie*, p. 225–264.
- Trappe, J., 1998, Phanerozoic phosphorite depositional systems: A dynamic model for a sedimentary resource system: Berlin, Springer-Verlag, *Lecture Notes in Earth Sciences* 76, 316 p.
- Trappe, J., 2000, Pangea: Extravagant sedimentary resource formation during supercontinent configuration, an overview: *Palaeogeography, Palaeoclimatology, Palaeoecology*, v. 161, p. 35–48.
- Van Cappellen, P., and Ingall, E.D., 1994, Benthic phosphorus regeneration, net primary production, and ocean anoxia: A model of the coupled marine biogeochemical cycles of carbon and phosphorus: *Paleoceanography*, v. 9, p. 677–692.
- Van Geen, A., McCorkle, D.C., Klinkhammer, G.P., 1995, Sensitivity of the phosphate-cadmium-carbon isotope relation in the ocean to cadmium removal by suboxic sediments: *Paleoceanography*, v. 10, p. 159–169.
- Visser, J.N.J., 1996, Post-glacial Permian stratigraphy and geography of southern and central Africa: boundary conditions for climatic modeling: *Palaeogeography, Palaeoclimatology, Palaeoecology*, v. 118, p. 213–243.
- Wardlaw, B.R., 1977, The biostratigraphy and paleoecology of the Gerster Limestone (Upper Permian) in Nevada and Utah: U.S. Geological Survey Open-File Report 77–470, p. 68.
- Wardlaw, B.R., 1980, Middle-Late Permian paleogeography of Idaho, Montana, Nevada, Utah, and Wyoming, in Fouch, T.D., and Magathan, E.R., eds., *Paleozoic paleogeography of the west-central United States: Rocky Mountain Paleogeography Symposium 1: Denver, Rocky Mountain Section of Society of Economic Paleontologists and Mineralogists*, p. 353–361.
- Wardlaw, B.R., 1995, Permian conodonts, in Scholle, P.A., Peryt, T.M., and Ulmer-Scholle, D.S., eds., *The Permian of northern Pangea, Volume 1: Paleogeography, paleoclimates, stratigraphy: Berlin, Springer-Verlag*, p. 186–195.
- Wardlaw, B.R., and Collinson, J.W., 1984, Conodont paleoecology of the Permian Phosphoria Formation and related rocks of Wyoming and adjacent areas, in Clark, D.L., ed., *Conodont biofacies and provincialism: Geological Society of America Special Paper 196*, p. 263–281.
- Wardlaw, B.R., Furnish, W.M., and Nestell, M.K., 1979, Geology and paleontology of the Permian beds near Las Delicias, Coahuila, Mexico: *Geological Society of America Bulletin*, v. 90, p. 111–116.
- Wardlaw, B.R., Snyder, W.S., Spinosa, C., and Gallegos, D.M., 1995, Permian of the western United States, in Scholle, P.A., Peryt, T.M., and Ulmer-Scholle, D.S., eds., *The Permian of northern Pangea, Volume 2: Sedimentary basins and economic resources: Berlin, Springer-Verlag*, p. 23–40.
- Westerlund, S.F.G., Anderson, L.G., Hall, P.O. J., Iverfeldt, A., Rutgers, L., Michiel, M., and Sundby, B., 1986, Benthic fluxes of cadmium, copper, nickel, zinc and lead in the coastal environment: *Geochimica et Cosmochimica Acta*, v. 50, p. 1289–1296.
- Wignall, P.B., and Twitchett, R.J., 1996, Oceanic anoxia and the end Permian mass extinction: *Science*, v. 272, p. 1155–1158.
- Yochelson, E.L., 1968, Biostratigraphy of the Phosphoria, Park City, and Shedhorn formations: U.S. Geological Survey Professional Paper 313-D, p. 571–660.
- Yugan, J., Jing, Z., and Qinghua, S., 1994, Two phases of the end-Permian mass extinction, in Embry, A.F., Beauchamp, B., and Glass, D.J., eds., *Pangea: Global environments and resources: Canadian Society of Petroleum Geologists Memoir 17*, p. 813–822.
- Xu, G., and Grant, R.E., 1994, Brachiopods near the Permian-Triassic boundary in South China: *Smithsonian Contributions to Paleobiology*, No. 76, p. 68.
- Zharkov, M.A., 1984, *History of Paleozoic salt accumulation: Berlin, Springer-Verlag*, 308 p.
- Ziegler, A.M., 1990, Phytogeographic patterns and continental configurations during the Permian period, in McKerrow, W.S., and Scotese, C.R., eds., *Paleozoic palaeogeography and biogeography: Geological Society [London] Memoir 12*, p. 363–379.